Article

Cell Reports

Periostin Activation of Integrin Receptors on Sensory Neurons Induces Allergic Itch

Graphical Abstract

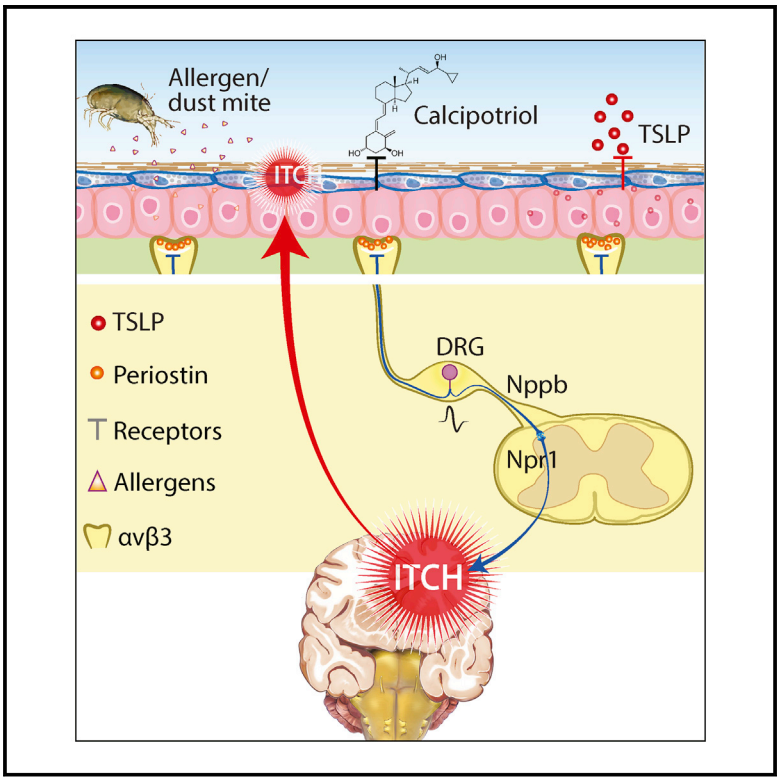

Authors

Santosh K. Mishra, Joshua J. Wheeler, Saumitra Pitake, ..., Ru-Rong Ji, Mei-Chuan Ko, Thierry Olivry

Correspondence

skmishra@ncsu.edu

In Brief

Mishra et al. demonstrate periostin-induced itch in mice, dogs, and monkeys and identify the integrin $\alpha_V\beta3$ as the periostin neuronal receptor. They find that keratinocytes release periostin in response to TSLP, thus identifying a possible reciprocal vicious circle implicating the cytokine TSLP and periostin in chronic allergic itch.

Highlights

- Periostin induces itch behavior in mice, dogs, and non-human primates
- Periostin directly activates sensory neurons through its integrin $\alpha_V\beta3$ receptor
- TSLP induces the secretion of periostin in keratinocytes via the JAK/STAT pathway
- A TSLP-periostin mutual activation loop might be involved in chronic allergic itch

Mishra et al., 2020, Cell Reports *31*, 107472
April 7, 2020
https://doi.org/10.1016/j.celrep.2020.03.036

CellPress

Cell Reports
Article

Periostin Activation of Integrin Receptors on Sensory Neurons Induces Allergic Itch

Santosh K. Mishra,[1,2,3,4,9,*] Joshua J. Wheeler,[1,2] Saumitra Pitake,[1] Huiping Ding,[5] Changyu Jiang,[7] Tomoki Fukuyama,[1] Judy S. Paps,[8] Patrick Ralph,[1] Jacob Coyne,[1] Michelle Parkington,[1] Jennifer DeBrecht,[1] Lauren C. Ehrhardt-Humbert,[1] Glenn P. Cruse,[1,2] Wolfgang Bäumer,[1,6] Ru-Rong Ji,[7] Mei-Chuan Ko,[5] and Thierry Olivry[2,8]

[1]Department of Molecular Biomedical Sciences, College of Veterinary Medicine, North Carolina State University, Raleigh, NC, USA
[2]Comparative Medicine Institute, North Carolina State University, Raleigh, NC, USA
[3]The WM Keck Behavioral Center, North Carolina State University, Raleigh, NC, USA
[4]Program in Genetics, North Carolina State University, Raleigh, NC, USA
[5]Department of Physiology and Pharmacology, Wake Forest School of Medicine, Winston-Salem, NC, USA
[6]Institute of Pharmacology and Toxicology, Department of Veterinary Medicine, Freie Universität Berlin, Berlin, Germany
[7]Duke University, Durham, NC, USA
[8]Department of Clinical Sciences, College of Veterinary Medicine, North Carolina State University, Raleigh, NC, USA
[9]Lead Contact
*Correspondence: skmishra@ncsu.edu
https://doi.org/10.1016/j.celrep.2020.03.036

SUMMARY

Chronic allergic itch is a common symptom affecting millions of people and animals, but its pathogenesis is not fully explained. Herein, we show that periostin, abundantly expressed in the skin of patients with atopic dermatitis (AD), induces itch in mice, dogs, and monkeys. We identify the integrin $\alpha_V\beta3$ expressed on a subset of sensory neurons as the periostin receptor. Using pharmacological and genetic approaches, we inhibited the function of neuronal integrin $\alpha_V\beta3$, which significantly reduces periostin-induced itch in mice. Furthermore, we show that the cytokine TSLP, the application of AD-causing MC903 (calcipotriol), and house dust mites all induce periostin secretion. Finally, we establish that the JAK/STAT pathway is a key regulator of periostin secretion in keratinocytes. Altogether, our results identify a TSLP-periostin reciprocal activation loop that links the skin to the spinal cord via peripheral sensory neurons, and we characterize the non-canonical functional role of an integrin in itch.

INTRODUCTION

Atopic dermatitis (AD)—also known as (atopic) eczema—is a common chronic allergic skin disease of humans and dogs with an estimated prevalence of up to 25% of children, a prevalence that depends on the patient's age, ethnic background, and geographical origin (Odhiambo et al., 2009). This condition often persists in adults (Abuabara et al., 2018). AD has a high impact on the health of patients because of an elevated risk of co-morbidities, such as arthritis, asthma, and allergic rhinitis (Eckert et al., 2017). Because AD is also associated with a high prevalence of anxiety, depression, and sleep disorders, there is an ensuing reduced quality of life and work productivity (Eckert et al., 2018). As a result, AD leads to substantial healthcare expenses for both patients and society (Adamson, 2017; Eckert et al., 2017).

In addition to the classic erythema and eczematous lesions with a characteristic age-related distribution, AD is associated with a chronic recurrent itch that is often moderate to severe (Shahwan and Kimball, 2017; Weidinger and Novak, 2016). The mechanism of atopic itch is complex, because it begins with the cutaneous release of a myriad of pruritogenic mediators, including histamine, neurotrophins, eicosanoids, proteases, and cytokines (reviewed in Bautista et al., 2014; Mollanazar et al., 2016; Storan et al., 2015; Voisin et al., 2017). Notable pruritus-inducing or pruritus-sensitizing cytokines are those typical of T helper type 2 (Th2) immune reactions, such as interleukin (IL) 4 and IL-13 (Cevikbas et al., 2014; Dillon et al., 2004; Oetjen et al., 2017) and thymic stromal lymphopoietin (TSLP) (Wilson et al., 2013).

Pruritogenic mediators secreted in the skin will generally bind to their respective receptors located on neurites of peripheral somatosensory neurons with a cell body located in the dorsal root ganglia (DRG) (reviewed in Bautista et al., 2014; Han and Dong, 2014; Mollanazar et al., 2016). These pruritogens will activate either G-protein-coupled receptors (GPCRs) (Nguyen et al., 2017; Wilson et al., 2011; Han et al., 2006; Imamachi et al., 2009) or IL (Cevikbas et al., 2014) or toll-like receptors (Liu and Ji, 2014), as well as transient receptor potential (TRP) channels on DRG sensory neurons to begin the transduction of the itch signal to the central nervous system (Imamachi et al., 2009; Kittaka and Tominaga, 2017; Shim et al., 2007). Similarly, sensory neurons appear to co-opt classic immune pathways to mediate chronic itch, which depends on neuronal IL-4Rα and JAK1 signaling (Oetjen et al., 2017). The next step in itch propagation is the release of neurotransmitters from the primary afferents in the spinal cord. Several neurotransmitters have been characterized that either excite and/or inhibit itch neurotransmission (Ma, 2014; Mishra and Hoon, 2013, 2015). Among them, the B natriuretic peptide (BNP), also known as natriuretic polypeptide B (NPPB), was identified and found to be expressed by the small subset of neurons in the DRG, which is involved in chemical-induced itch. Thus, NPPB-expressing DRG neurons are believed

to be the (inflammatory) itch neurons in the DRG (Mishra and Hoon, 2013). Recently, somatostatin (SST) was also shown to be expressed in itch-transmitting DRG neurons, of which nearly all also secrete NPPB (Huang et al., 2018). These findings have significantly improved our understanding of the itch sensation in mice and humans, but we are still far from being able to successfully and completely treat this noxious sensation associated with many cutaneous and neurologic diseases (Carstens, 2008; Oaklander, 2011; Paus et al., 2006; Yosipovitch and Samuel, 2008).

Periostin is a fasciclin extracellular matrix (ECM) protein that exerts its function after binding to cell-surface receptors of the integrin family that include $\alpha_V\beta3$ and $\alpha_V\beta5$ (Izuhara et al., 2017). After stimulation with various stimuli, including transforming growth factor β (TGF-β) and the Th2 cytokines IL-4 and IL-13, periostin is secreted by at least three types of cells, including fibroblasts, epithelial cells, and endothelial cells (Izuhara et al., 2017; Masuoka et al., 2012). Because of its fibroblast-rich environment, periostin is highly expressed in the skin, where its strongest immunostaining is found at the dermoepidermal junction (Yamaguchi, 2014). Periostin appears to be critical to the granulation and remodeling stages of cutaneous wound healing, because it promotes the differentiation and migration of fibroblasts and the proliferation of keratinocytes (Yamaguchi, 2014). Furthermore, periostin was found to be expressed in several disease states in which fibrosis is observed, for example, hypertrophic scars, bronchial asthma, pulmonary and systemic fibrosis, and psoriasis (Yamaguchi, 2014). Periostin is also produced in the skin of both humans (Kou et al., 2014) and dogs with spontaneous AD (Merryman-Simpson et al., 2008; Mineshige et al., 2015). This fibrogenic cytokine is upregulated after epicutaneous allergen challenges in mouse (Masuoka et al., 2012; Shiraishi et al., 2012) and dog (Olivry et al., 2016) models of AD; in the latter, it is transcribed late, after an epicutaneous allergen provocation (Olivry et al., 2016). In humans with AD, serum levels of periostin not only correlate with disease activity but also appear to reflect the chronicity of the disease, because its levels are highest when skin lichenification (thickening) is present (Kou et al., 2014). Because periostin induces the secretion of the Th2 cytokine-promoting TSLP by keratinocytes (Shiraishi et al., 2012), an amplification loop involving periostin (i.e., periostin → TSLP → Th2 cytokines → periostin) is a mechanism suspected to lead to the dermal remodeling and epidermal hyperplasia typical of chronic AD (Masuoka et al., 2012; Shiraishi et al., 2012; Takahashi et al., 2016).

Because of the likely role of periostin in the pathogenesis of chronic skin lesions of AD, we wondered whether it might also induce pruritus in this disease. Herein, we characterize the pruritogenic potential of periostin when injected into the skin of three mammalian species. We confirm, using molecular, pharmacological, cellular, and physiological assays, that periostin can directly activate the sensory neurons via integrin $\alpha_V\beta3$, whose removal or inhibition reduces the pruritogenic effect of its ligand. Finally, we show that TSLP, MC903, and house dust mites (HDMs) all induce the expression and secretion of periostin in keratinocytes, thereby confirming the possibility of a TSLP-induced periostin release by epidermal cells, which might induce not only chronic inflammation but also itch.

RESULTS

Periostin Induces Itch in Mice, Dogs, and Monkeys

Because periostin is produced in large amounts in the skin of patients suffering from pruritic dermatoses such as AD and psoriasis (Merryman-Simpson et al., 2008; Mineshige et al., 2018), we speculated its possible role as a pruritogen. Therefore, we first tested whether intradermal (i.d.) injections of periostin triggered itch behavior in mice. Surprisingly, a single injection of periostin in the dorsal neck of mice induced robust scratching behavior within 15 min of an intracutaneous injection (Figure 1A). Because somatosensory neurons are involved in itch, pain, and touch, we then used the cheek injection model that is known to permit the discrimination of pain and itch behaviors in mice (Kardon et al., 2014; Shimada and LaMotte, 2008). Interestingly, periostin injections in the cheek caused robust scratching behavior similar to that of histamine, whereas it did not induce wiping when compared with capsaicin, the archetypal pain inducer in mice (Figures S1A and S1B). We then verified whether periostin induced pain behavior by directly applying it into the cornea, because only nociceptive compounds, such as capsaicin, induce a wiping behavior when added to the eye of mice (Mishra and Hoon, 2010). We found no eye-wiping response to the ocular application of periostin, while capsaicin caused robust eye-wipe behavior in wild-type mice compared with TRPV1 knockout mice (Figure S1C).

Many exogenous and endogenous molecules—for example, histamine—have been shown to induce itch in mice, but except for IL-31, most of them are not conserved pruritogens among animal species or humans (Olivry and Bäumer, 2015). Recombinant mouse periostin has an approximately 85% and 90% amino acid homology with that of monkeys and dogs, respectively. To assess whether periostin induced itch in these higher mammalian species, we injected mouse recombinant periostin (25 μg/100 μL i.d.) in dogs and subcutaneously (s.c.) in monkeys. Excitingly, we found that periostin induced robust scratching within 15 min of injection, irrespective of the route (intracutaneous or s.c.) and body site (neck or thigh) of administration; meanwhile, injections of their control had no influence on itch manifestations (Figures 1B and 1C). Altogether, these results show that periostin acts as a strong pruritogen with a behavioral response that is conserved among mice, dogs, and monkeys.

Because many mediators derived from several immune cell types can activate sensory neurons to induce itch, we wondered whether the periostin-induced pruritus occurred because of direct (primary) or indirect (secondary) stimulation of sensory neurons. To determine whether the periostin-induced itch followed mast cell activation, we challenged deoxyribonucleoprotein (DNP)-specific immunoglobulin E (IgE)-sensitized mast cells with increasing concentrations of the hapten DNP or periostin. As expected, DNP induced the degranulation of mast cells sensitized with anti-DNP IgE, but periostin did not (Figures S1D and S1E). Furthermore, we did not observe periostin-dependent change in calcium release when mast cells were directly stimulated with periostin alone, and there was no enhancement of the DNP-induced calcium responses after the addition of periostin to DNP-sensitized mast cells (Figure S1F). Similarly, to exclude the possibility that the stimulation of skin resident or infiltrating immune cells by periostin could release mediators that would indirectly stimulate

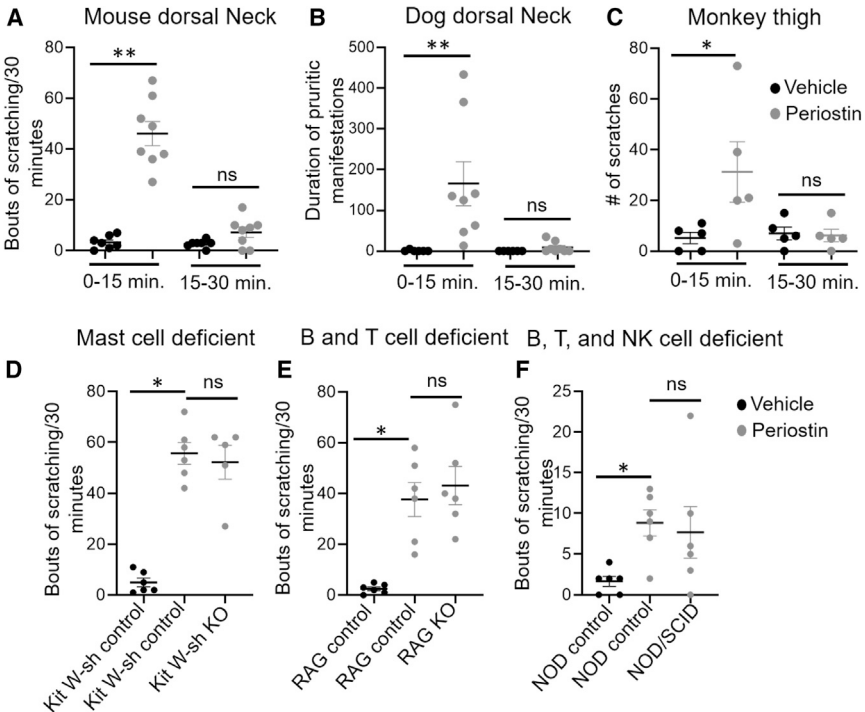

Figure 1. Periostin Induces Robust Itch Behavior Mediated via Somatosensory Neurons

(A) Scratching bouts following an i.d. injection of vehicle (20 μL PBS, black circle) or periostin (5 μg/20 μL, gray circle) into the dorsal neck of wild-type C57BL/6J mice. Mice scratching bouts were recorded for 0–15 and 15–30 min. Periostin induced significant scratching bouts in 0–15 min compared with 15–30 min. We observed no change in vehicle response between 0–15 and 15–30 min. n = 7–8 mice per group.

(B) i.d. injection of periostin (25 μg/100 μL, gray circle) or vehicle (100 μL PBS, black circle) in the dorsal neck of dogs. Durations of pruritus manifestations (DPMs) were measured first for 0–15 min and second for 15–30 min. Periostin induced significant DPMs in 0–15 min compared with 15–30 min. We found no change in vehicle response between 0–15 and 15–30 min. n = 8 dogs per group.

(C) s.c. injection of periostin (25 μg/100 μL, gray circle) or vehicle (100 μL PBS, black circle) in the thigh of monkeys. The number of scratches were recorded for 0–15 and 15–30 min. Periostin induced significant scratching responses in 0–15 min compared with 15–30 min. There was no change in vehicle response between 0–15 and 15–30 min. n = 5 monkeys per group.

(D) Scratching bouts following i.d. injection of vehicle (20 μL PBS, black circle) or periostin (5 μg/20 μL, gray circle) in the dorsal neck of control and mast-cell-deficient mice. There was no change in periostin-induced scratching behaviors between control and mast-cell-deficient mice. n = 5–6 mice per group.

(E) Scratching bouts following a i.d. injection of vehicle (20 μL PBS, black circle) or periostin in the dorsal neck of control and B and T cell-deficient mice (5 μg/20 μL, gray circle). We observed no change in periostin-induced scratching behaviors between control and B and T cell-deficient mice. n = 6 mice per group.

(F) Scratching bouts following i.d. injection of vehicle (20 μL PBS, black circle) or periostin (5 μg/20 μL, gray circle) in the dorsal neck of control and B, T, and NK cell-deficient mice. There was no change in periostin-induced scratching behaviors between control and mutant mice. n = 6 mice per group.

All data were presented as the mean ± SEM in mice, dogs, and monkeys. One-tailed Student's t test was performed between two groups to determine significance (*$p < 0.05$, **$p < 0.01$).

somatosensory neurons and cause itch, we injected periostin into the neck of mice deficient in mast cells (Kit W-sash) (Grimbaldeston et al., 2005), B and T cells (Rag1$^{-/-}$), and B, T, and NK cells (non-obese diabetic/severe combined immunodeficiency [NOD/SCID]) (Bosma et al., 1983; Mombaerts et al., 1992; Shultz et al., 1995); we then compared the induced itch response with that of control littermates. We detected similar scratching bouts in the mast-cell-, B and T cell-, or B, T, and natural killer (NK) cell-deficient and control mice (Figures 1D–1F). Altogether, these data suggest that periostin-evoked itch does not specifically require mast cells, lymphocytes, or pruritogens released when these cells are activated. In contrast, our results lead to the hypothesis that periostin might induce itch via the direct activation of somatosensory neurons.

Integrin Receptors for Periostin Are Present in DRG Somatosensory Neurons

Periostin has been shown to bind to the heterodimeric $\alpha_V\beta3$, $\alpha_V\beta5$, and $\alpha IIb\beta3$ integrins (Gillan et al., 2002; Li et al., 2010; Ruan et al., 2009). Hence, we investigated the expression of α_V, β3, β5, and αIIb homomers in DRG sensory neurons. We found, using qRT-PCR, that these integrin subunits are consistently expressed in mice, dog, and monkey DRGs (Figures 2A–2C). By using immunohistochemistry (IHC) in mice, we found that the α_V and β5 subunits are expressed in almost all DRG neurons (Figure S2), whereas only a small subset of such neurons expressed the integrin β3 subunit, along with the itch neurotransmitter SST (Figure 2D). Because only a small percentage of DRG neurons can transmit itch, we focused our subsequent studies on the $\alpha_V\beta3$ integrin.

We have shown that the DRG somatosensory neurons responsible for itch transmission co-express both NPPB and SST (Huang et al., 2018). To assess whether these itch-specific neurons also expressed the periostin receptor of interest, we used SST-cre::tdTomato mice that exclusively have the red Tomato protein in SST- and NPPB-positive neurons. Therefore, we performed IHC using an antibody against the β3 integrin homomer. Our results confirmed the expression of β3 in SST/NPPB-expressing DRG neurons. Indeed, 93% of these SST-positive neurons were positive for β3 (135 of 145 cells), whereas only 4% of the β3-positive neurons were negative for SST (6 of 145 cells). Similarly, only 3% of SST/NPPB-positive cells were β3 negative (4 of 145 cells), as shown in Figure 2E. Altogether, these observations indicate that the integrin $\alpha_V\beta3$ is expressed in a subset SST/NPPB-expressing DRG sensory neurons known to transduce inflammatory itch (Usoskin et al., 2015).

Periostin Directly Activates Itch-Transmitting DRG Somatosensory Neurons

Somatosensory neurons in the DRG express receptors for the pruritogens that activate them (Han et al., 2006, 2013; Imamachi

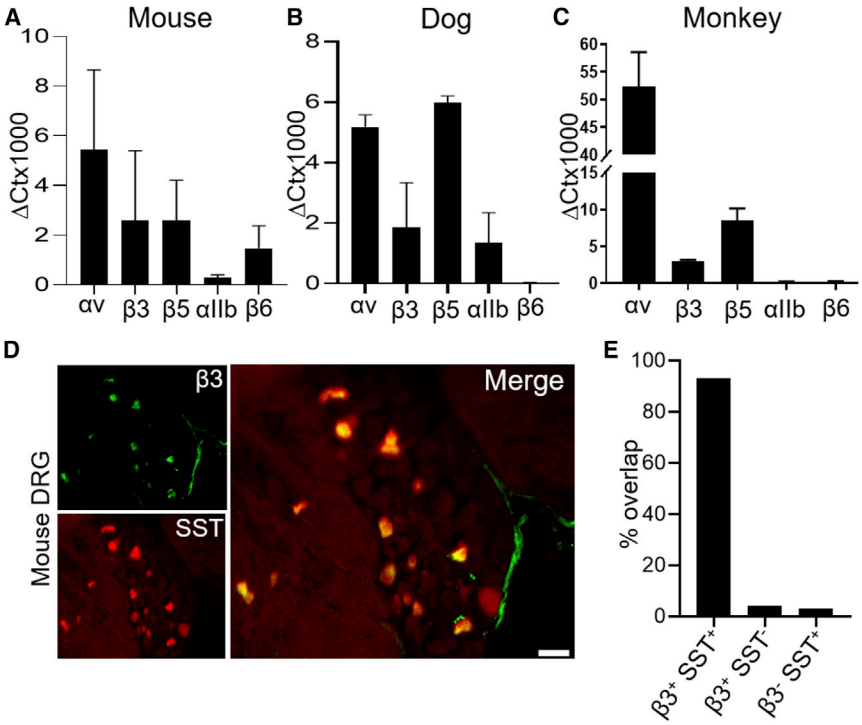

Figure 2. Periostin Integrin Receptor Subunits Are Expressed in DRG Sensory Neurons

(A–C) qRT-PCR was used to quantify the expression of subunits of integrin receptors relative to glyceraldehyde 3-phosphate dehydrogenase (GAPDH) in the DRG of 4 mice (A), 3 dogs (B), and 5 non-human primates (C). A minimum of two technical replicates were performed for mice and dogs, and three technical replicates were performed for non-human primate.

(D) Co-expression of the integrin receptor β3 subunit (green) and SST-tdTomato (red) in DRG neurons. Scale bar, 75 μm.

(E) Both SST-tdTomato and integrin β3 were quantified for overlapping and non-overlapping populations. n = 3 mice, with an average of 3 sections per mouse.

All data in (A)–(C) were presented as mean ± SEM.

et al., 2009). To investigate whether periostin directly activates DRG sensory neurons, this cytokine was applied to cultured DRG sensory neurons loaded with the calcium chelating dye Fura-2AM (fura 2-acetoxymethyl ester). We first measured the response of DRG sensory neurons to several concentrations of periostin. We found an equal number of cells responding to periostin at 8, 16, and 32 ng/μL (Figure S3). Hereafter, we used periostin at 16 ng/μL throughout our study to measure the calcium influx in DRG neurons. Periostin led to the entry of calcium into neurons that similarly responded to the TRPA1 agonist allyl isothiocyanate (AITC) (mustard oil) and TRPV1 agonist capsaicin (Figure 3A). In parallel, we observed an increase in amplitude in response to periostin in neurons that also reacted to the TRPV1-activating capsaicin, TRPA1-activating mustard, and potassium chloride (KCl; Figure 3B). Periostin-dependent changes in intracellular calcium were observed in about 10% ± 2% of DRG sensory neurons (Figure 3C).

Next, we wondered whether the periostin-associated activation of DRG neurons involved the influx of extracellular or intracellular calcium. The removal of extracellular calcium silenced this neuronal activation induced by periostin (Figure 3D). Moreover, the intracellular signaling proteins PLC and/or Gβγ did not appear involved in this calcium response, because the use of their respective inhibitors did not diminish the neuronal activation by periostin (Figure 3E). Altogether, these results indicate that extracellular calcium is involved in the periostin-induced neuronal activation.

We then isolated and cultured mouse DRG neurons and separated the itch-transmitting neurons that expressed SST (shown with arrowheads in Figure 3F). Our pilot data had shown weak inward currents at 1 μg/mL; therefore, we used 10 μg/mL in our subsequent experiment. Using patch clamping, these SST-positive neurons directly responded to periostin with an inward current (Figure 3F), but SST-negative neurons had no response to periostin. In summary, we showed herein the direct activation of SST-expressing itch-transmitting neurons by periostin and that this involved the entry of extracellular calcium to cause an inward current into the neurons that also expressed TRPV1.

Lastly, previous studies have shown that TSLP and IL-31 transduce itch signals via their respective receptors on sensory neurons (Cevikbas et al., 2014; Wilson et al., 2013). To determine the overlap of the neurons activated by these pruritogens and periostin, we assessed the ratiometric calcium response of DRG neurons to periostin, IL-31, and TSLP. We calculated the percentage of overlapping cells by counting the neurons responding to both periostin and either TSLP or IL-31 with neurons normalized to the periostin response. We found that 16% of TSLP-responding neurons did so with periostin (35 cells with TSLP/225 cells with periostin) and about 38% of IL-31-activated neuron overlapped with those responding to periostin (85 cells with IL-31/225 cells with periostin). Altogether, these results suggest the existence of populations of neurons responding to periostin that overlap partially with those activated by the allergic pruritogenic cytokines TSLP and IL-31.

The Blocking of Integrin $\alpha_V\beta3$ on DRG Sensory Neurons Inhibits the Calcium Influx and Periostin-Induced Itch

First, we examined the effect of the broad integrin receptor antagonist cilengitide on DRG sensory neurons. Cilengitide is a potent antagonist of both $\alpha_V\beta3$ and $\alpha_V\beta5$ with low IC_{50} (half maximal inhibitory concentration) in the nanomolar range (3 and 37 nM, respectively) (Goodman et al., 2002). To examine whether cilengitide inhibited periostin-induced calcium responses, neurons were perfused with a buffer containing 100 nM of this antagonist. The periostin-dependent calcium response was significantly reduced during cilengitide perfusion (Figure 4A), thereby demonstrating that integrins are involved

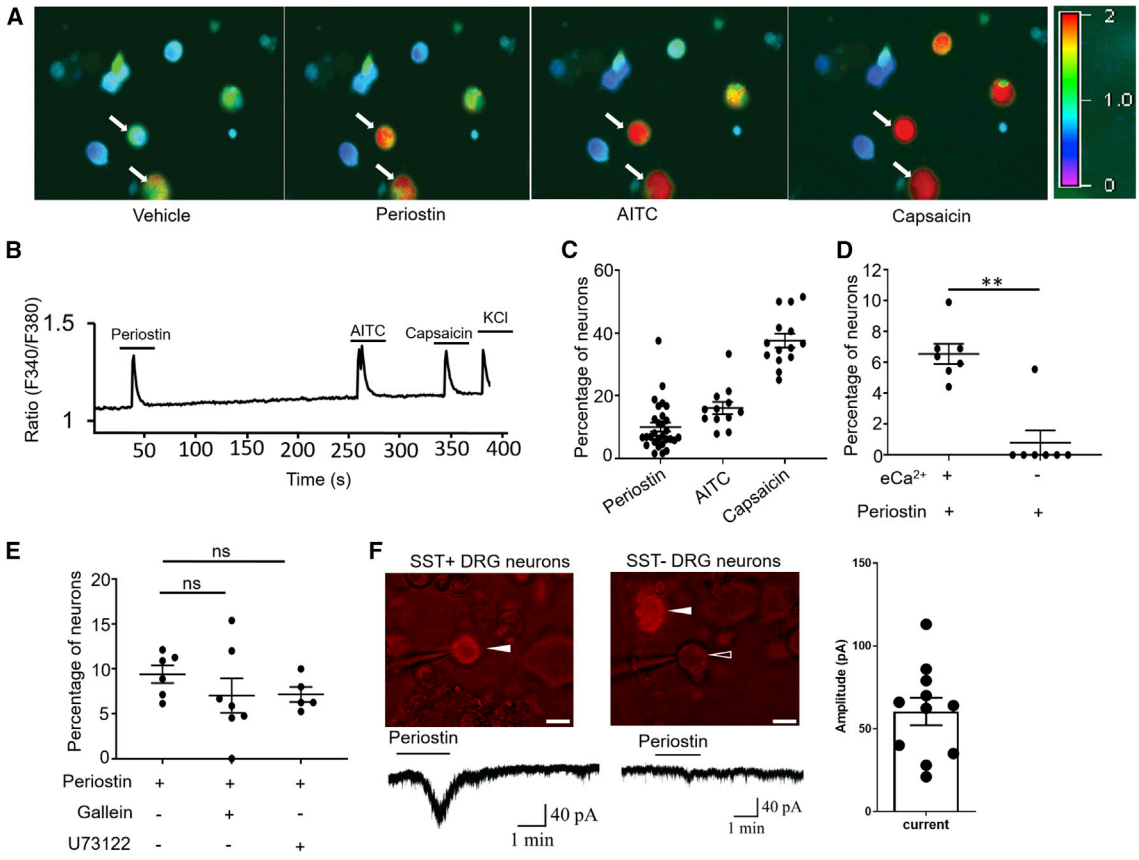

Figure 3. Periostin Directly Activates DRG Sensory Neurons

(A) DRG neurons were pre-incubated (30 min) with the calcium dye Fura-2AM (5 μM), and the calcium influx was measured by exciting cells with alternating 340/380 nm wavelengths. Arrows indicate cells responding to periostin, AITC mustard (TRPA1 agonist), and capsaicin (TRPV1 agonist).

(B) Recording showing the amplitude of cytosolic Ca^{2+} increase for a single region of interest taken every 100 ms.

(C) Periostin-induced calcium response in DRG neurons treated with periostin (16 ng/μL), AITC mustard (100 μM), and capsaicin (1 μM). n ≥ 6 mice.

(D) There were no neuronal calcium responses to periostin in the absence of extracellular calcium. n = 3 mice.

(E) Periostin-induced calcium response was not affected by either the Gβγ blocker gallein (100 μM) or the phospholipase C inhibitor U73122 (1 μM). n = 2 mice.

(F) SST-positive small-diameter neurons (white arrowhead in the left panel) were patched, and the inward current was measured in response to periostin (10 μg/mL). The SST-positive neuron produced an inward current to periostin, suggesting the presence of the $\alpha_V\beta3$ integrin receptor on SST-positive cells. In the right panel, we showed the SST-negative neuron (blank arrowhead) did not respond to periostin (10 μg/mL). SST-positive neurons are a small subset of TRPV1-expressing neurons. In 11 SST-positive neurons, the average current induced by periostin was 58.4 pA (column bar). Nine SST-negative neurons showed no current amplitude in response to periostin. n ≥ 4 mice. Scale bar, 20 μm.

A dot point in the calcium imaging scatterplot represents one coverslip. All data were presented as mean ± SEM, and the significance differences between two groups were determined by unpaired Student's t test (**p ≤ 0.01).

in such calcium influx. Importantly, the perfusion with cilengitide did not reduce either AITC or capsaicin-induced calcium responses on DRG sensory neurons (Figure 4A). However, which of the two cilengitide-inhibited integrins was specifically involved in the periostin-induced calcium response in sensory neurons was not determined by this experiment.

Next, we wanted to assess whether the periostin-induced itch behavior in mice would also be affected by the dual integrin inhibitor cilengitide. We first injected cilengitide into mice and confirmed that alone, it did not induce itch behavior. We then injected cilengitide intravenously (i.v.) and intraperitoneally (i.p.) 10 min before periostin i.d. injection. Finally, we mixed periostin and cilengitide together and injected it s.c. Altogether, the periostin-induced itch behavior was significantly reduced when periostin was administered after or with cilengitide by all three routes of injections (Figure 4B), and the strongest inhibitory effect of cilengitide was seen after i.v. pre-injections of this antagonist.

Integrin β3, TRPV1, TRPA1 and NPPB Mediate the Periostin-Induced Itch

The α-integrin subunit of the $\alpha_V\beta3$ heterodimer is expressed in nearly all DRG neurons (Figure S2). Because most cells responding to periostin are activated by the TRPV1 agonist capsaicin, we suspected that the integrin $\alpha_V\beta3$-expressing neurons are a subset of those that have TRPV1. We thus generated a conditional knockout of β3 subunits from a subset of TRPV1-expressing neurons by crossing a β3-flox mouse with a mouse that expresses the Cre recombinase in its TRPV1-lineage neurons

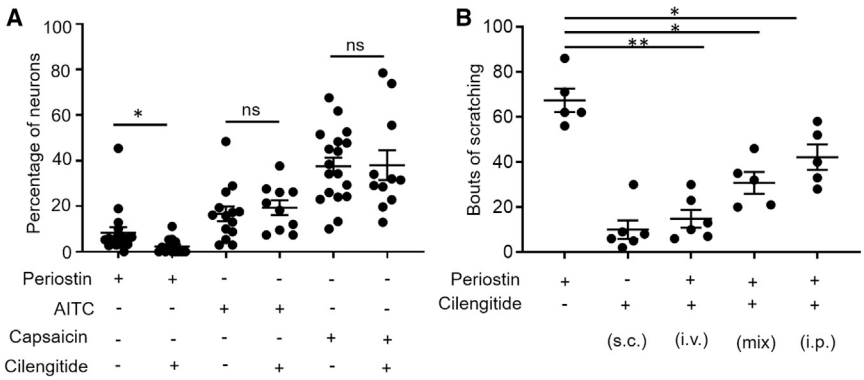

Figure 4. Pharmacological Blockage of Integrin Receptors Inhibits Both Calcium Influx and Periostin-Evoked Itch Behavior

(A) Cilengitide (100 nM), a non-specific blocker for integrin receptors $\alpha_V\beta3$ and $\alpha_V\beta5$, inhibits the periostin-induced calcium response, but it had no effect on the mustard- or capsaicin-induced response. n = 4–5 mice, and each data point represents one coverslip.

(B) Injections of periostin (5 μg/20 μL) following the co-administration of cilengitide by different routes (100 nM) in mice. n = 5–6 mice each group.

All data were presented as mean ± SEM, and the significance differences between two groups were determined by unpaired Student's t test (*$p \leq 0.05$, **$p \leq 0.01$).

(Mishra et al., 2011). We confirmed by IHC that the β3 subunit was knocked out from the TRPV1-cre::$\beta3^{-/-}$ mutant mice (Figure 5A) with an almost 95% reduction in expression (Figure 5B). Because our immunostaining revealed that the β3 integrin was expressed in SST-positive itch neurons (Figure 2D), this integrin was conditionally knocked out of TRPV1-expressing DRG neurons (Mishra et al., 2011). We observed a significant reduction in the calcium response to periostin in these neurons; however, we did not find change in the calcium influx generated by capsaicin (Figure 5C) suggesting these mice have no developmental defect in TRPV1-expressing neurons. We then i.d. injected TRPV1-cre::$\beta3^{-/-}$ mice with periostin (Figure 5D), histamine (Figure 5E), and chloroquine (Figure 5F). TRPV1-cre::$\beta3^{-/-}$ mice had no significant changes in histamine- and chloroquine-induced scratching bouts when compared with their control littermates. Conversely, TRPV1-cre::$\beta3^{-/-}$ mice injected with periostin exhibited a significant near-complete reduction in scratching behavior when compared with their control littermates, confirming that the observed decrease in itch depended on β3. To examine whether the integrin receptor β3 was also important for the pain and touch sensations, we used standard behavioral assays to measure acute pain in TRPV1-cre::$\beta3^{-/-}$ and compared the results with those of experiments done with control littermates. TRPV1-cre::$\beta3^{-/-}$ mice showed no apparent differences in responses to thermal stimuli (both hot and cold) or mechanosensation, and they had normal motor function (Figures 5G–5J).

Because the neuronal calcium response induced by the histamine and chloroquine pruritogens depends on TRP channels after activation of their respective receptors, we examined the role of both TRPA1 and TRPV1 channels in the periostin-induced calcium response. We first showed that periostin-responsive neurons overlapped with those responding to AITC (mustard oil) and capsaicin (Figures 3A and 3B). We then demonstrated that the periostin-dependent neuronal calcium response was significantly decreased in TRPV1$^{-/-}$ and TRPA1$^{-/-}$ and that the decrease was highest in TRPV1$^{-/-}$/TRPA1$^{-/-}$ double-knockout mice (Figure 6A). Altogether, these results confirm that the neurons activated by periostin use TRPV1 and TRPA1 synergistically. Because both TRPV1 and TRPA1 ion channels are involved in transducing itch behavior *in vivo* (Cevikbas et al., 2014; Imamachi et al., 2009; Lagerström et al., 2010; Mishra et al., 2011; Sheahan et al., 2018; Wilson et al., 2011, 2013), we examined whether the periostin-induced itch required either one or both of these TRP channels and found that it was significantly diminished in TRPV1 (Figure 6B) and TRPA1 (Figure 6C) single-knockout mice and TRPV1/TRPA1 double-knockout mice (Figure 6D).

Finally, we examined whether the itch-transmitting neuropeptide NPPB, which is expressed in a small subset of TRPV1-expressing neurons, was also involved in periostin-induced itch. As expected, we found a significant reduction in scratching bouts in mice deficient in NPPB compared with control animals (Figure 6E). Altogether, our results suggest the involvement of both TRPV1 and TRPA1 ion channels downstream of activated integrin $\alpha_V\beta3$, with TRPV1 neurons releasing NPPB as a neuropeptide to transmit the pruritogenic signal to spinal cord interneurons.

Keratinocytes Release Periostin in Response to the Cytokine TSLP

In diseases such as AD, keratinocytes contribute to the initial inflammatory response through the release of many neurostimulatory mediators that include the Th2 cytokine TSLP (Wilson et al., 2013). We first verified that mouse keratinocytes have a functional TSLP receptor (TSLPR) and IL-7α receptor (TSLPR/ILR7α) complex (Figure S4A) in response to TSLP (2 ng/mL) and that they expressed TSLPR protein in both the mouse keratinocyte cell line and in skin lysates (Figure S4B). Then, we showed that TSLP-stimulated keratinocytes induced the release of periostin *in vitro* (Figure 7A). This TSLP-induced periostin release was blocked by the JAK2 inhibitor SD 1008 and the STAT3 inhibitor niclosamide, thereby implicating the JAK/STAT pathway downstream of the TSLPR in the production and release of periostin by keratinocytes in response to TSLP (Figure 7B). We then found that TSLP induced both phosphorylated STAT3 (pSTAT3; Figure 7C) and its ensuing translocation into the nucleus of mouse keratinocytes depicted by non-visible DAPI (4′,6-diamidino-2-phenylindole) nuclear staining because of pSTAT3 on cells treated with TSLP (Figure S4C, ix and x) compared with vehicle control (Figure S4C, iv and v). Surprisingly, even though STAT5 and STAT6 are involved in the IL-31 atopic itch cytokine pathway (Hermanns, 2015; Park et al., 2012), we did not detect change in either of these transcription factors in response to TSLP keratinocyte stimulation (Figure S4D). Finally, we examined whether TSLP induced the

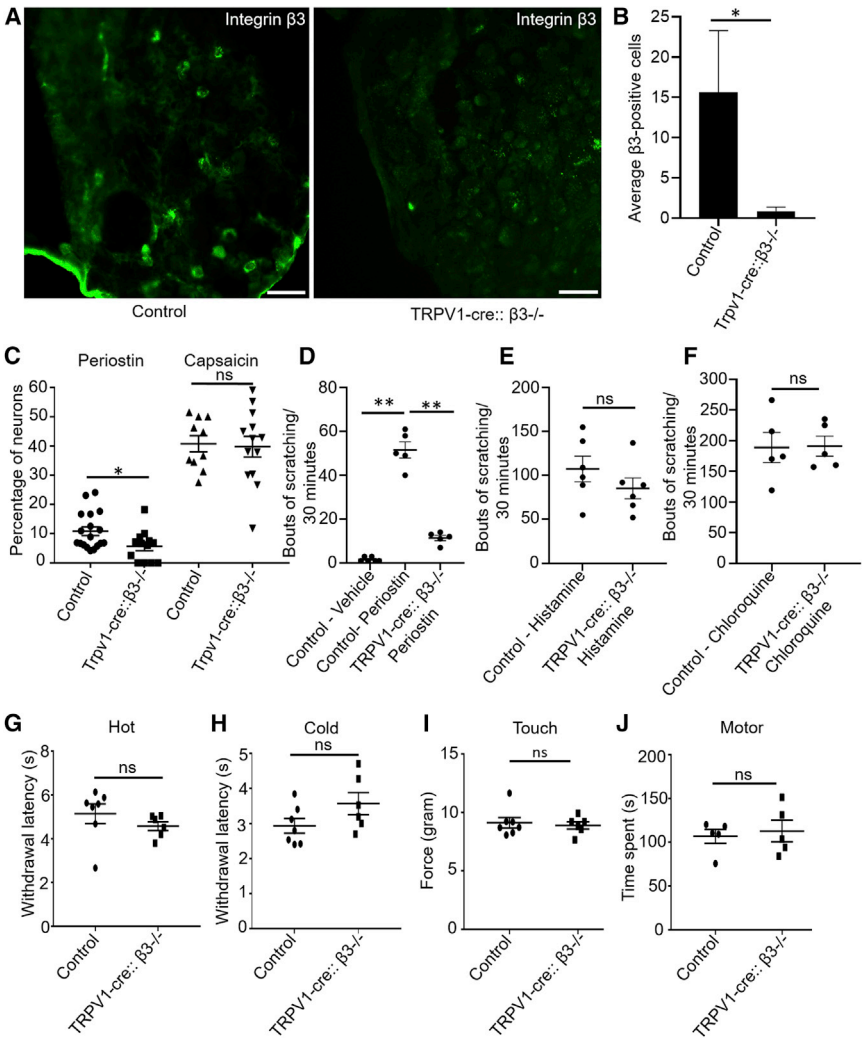

Figure 5. The Periostin-Mediated Itch Behavior Implicates the Integrin Receptor $\alpha_V\beta3$ in TRPV1-Expressing Neurons

(A) IHC showed the elimination of β3 in TRPV1-cre::$\beta3^{-/-}$ mice compared with either TRPV1-cre or $\beta3^{fl/fl}$ alone as control. Scale bar, 75 μm.

(B) Quantification of β3-immunopositive cells of DRGs from the TRPV1-cre::$\beta3^{-/-}$ mice demonstrated a significant reduction compared with control littermates ($\beta3^{fl/fl}$). n = 3–4 mice, and an average of 3 sections from each mice was quantified.

(C) Periostin-mediated calcium response is reduced in TRPV1-cre::$\beta3^{-/-}$ mice, but there was no change in the capsaicin-induced calcium influx. n = 3–4 mice, and each data point represents one coverslip.

(D) Itch behavior following the injection in the nape of the neck of vehicle (PBS) or periostin in control and mutant (TRPV1-cre::$\beta3^{-/-}$) mice. Periostin-induced itch was significantly reduced in mutant mice compared with control littermates. n = 5–6 mice per group.

(E) Itch response to i.d. injection of histamine in control littermates and mutant (TRPV1-cre::$\beta3^{-/-}$) mice remained normal. n = 6 mice per group.

(F) Itch response to i.d. injection of chloroquine in control and TRPV1-cre::$\beta3^{-/-}$ mice remained normal. n = 5 mice per group.

(G) Hargreaves assays between control and mutant (TRPV1-cre::$\beta3^{-/-}$) littermates. Both control and mutant mice had a normal withdrawal latency. n = 6–7 per group

(H) Dry-ice cold assays between control and mutant (TRPV1-cre::$\beta3^{-/-}$) littermates. Both control and mutant mice showed normal behavior responses. n = 6–7 per group

(I) Touch (von Frey) tests between control and mutant (TRPV1-cre::$\beta3^{-/-}$) littermates. Both control and mutant mice demonstrated normal behavior responses. n = 6–7 per group

(J) Rotarod test shows motor deficits between control and mutant (TRPV1-cre::$\beta3^{-/-}$) littermates. Both control and mutant mice had normal behavior responses. n = 5 per group.

All data were presented as mean ± SEM. One-way ANOVA Dunn's test was performed for equal or more than three groups (**$p < 0.001$), and unpaired Student's t test was performed to determine significance (*$p \leq 0.01$).

release of periostin *in vivo*. We established that the s.c. injection of TSLP into the neck of mice caused a significant increase in local cutaneous levels of periostin, which was accompanied by the production of pSTAT3 (Figures 7C–7E). Altogether, these results confirmed the involvement of the JAK/STAT pathway in TSLP-induced periostin production and release *in vivo*.

Periostin Is Involved in Chronic Allergic Itch

Mice treated with the vitamin D3 analog calcipotriol (MC903) develop itch, skin lesions, and a rise in IgE levels resembling those of humans with extrinsic AD (Moosbrugger-Martinz et al., 2017). Importantly, these changes do not depend on mouse gender or on genetic background. We used C57BL/6 mice and topically applied MC903 once daily for 7 days. This application led to chronic AD-like skin changes (Figure 7F) and elevated skin levels of periostin (Figures 7G and 7H). The topical application of MC903 to both β3-alone (control) and TRPV1-cre::$\beta3^{-/-}$ mutant mice had a day-dependent increase in skin thickness compared with their control treated with vehicle (ethanol) (Figure 7I). In contrast, MC903 applied to the dorsal neck of control mice induced significant scratching bouts that were attenuated in TRPV1-cre::$\beta3^{-/-}$ mutant mice (Figure 7J).

Finally, we sensitized NC/NgA mice to *Dermatophagoides farinae* HDMs and then repeatedly challenged them with this ubiquitous and potent allergen. The topical application of HDMs on mouse dorsal skin led to elevated skin levels of periostin compared with those of mice treated with the vehicle (mineral oil; Figure S5A). As expected, periostin skin levels were reduced significantly after treatment with the glucocorticoid betamethasone dipropionate (Figure S5A). Similarly and in parallel, HDMs induced robust scratching behavior compared with untreated controls and betamethasone dipropionate reduced such

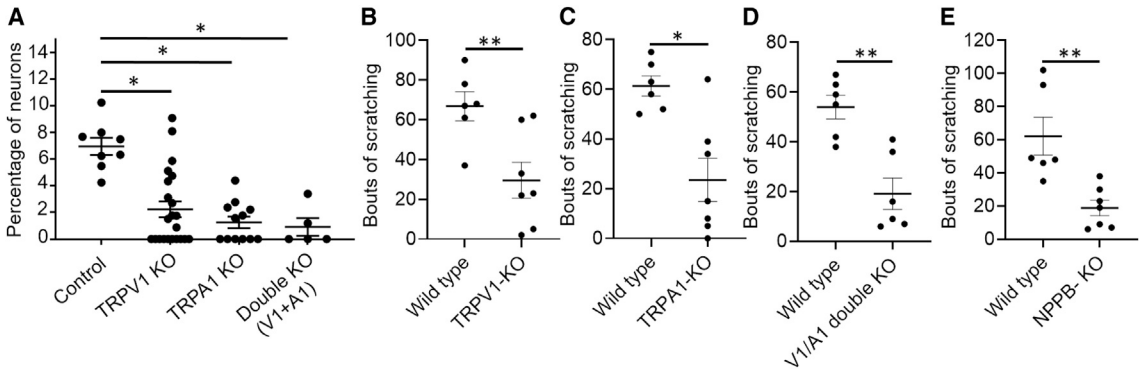

Figure 6. The Periostin-Mediated Calcium Influx Involves the Downstream Activation of TRP Channels and Periostin-Evoked Itch Dependent on TRP Channels and Neuropeptide NPPB

(A) Periostin-induced calcium response was inhibited in TRPV1, TRPA1, and double-knockout (KO) mice. The percentage of neurons that responded to periostin was normalized with KCl (1 mM). n = 3–4 mice, and each data point represents one coverslip. A minimum of two technical replicates were performed.

(B) i.d. injection of periostin in the dorsal neck of control littermates and TRPV1 KO mice. A significant reduction in itch behavior was observed in TRPV1 KO mice compared with control littermates. n = 5–7 mice per group.

(C) Significant reduction in itch behavior in TRPA1 KO mice compared with control littermates. n = 6 mice per group.

(D) Double-KO (TRPV1 + TRPA1) mice compared with control littermates showed reduced itch behavior. n = 6 mice per group.

(E) Significant reduction in itch behavior in NPPB KO mice compared with control littermates. n = 6–7 mice per group.

All data were presented as mean ± SEM, Significance was determined by unpaired Student's t test (*p = 0.01, **p $\leq$ 0.008).

scratching (Figure S5B). Overall, our results suggest that periostin is one of the endogenous cutaneous pruritogens involved in the itch that develops in the MC903 and HDM chronic allergic mouse models.

In summary of the results of the experiments reported earlier, we logically propose a model of periostin-integrin $\alpha_V\beta3$-TRPV1/TRPA1-NPPB activation that links the skin and sensory neurons and could explain the itch behavior during the chronic stages of allergic skin diseases in mice and perhaps other species (Figure 7K).

DISCUSSION

Herein, we show that periostin induces itch behavior by binding to the integrin $\alpha_V\beta3$ in a subset of itch-transmitting neurons that also express SST. We provide evidence supporting our hypothesis that periostin is an important pruritogen for chronic allergic itch. First, we established that periostin induced itch behavior in three species (mice, dogs, and monkeys), thereby suggesting an evolutionarily conserved pathway. We then showed that in mice, the periostin-induced itch behavior was independent of mast cells, T cells, B cells, and NK cells. We demonstrated that the integrin $\alpha_V\beta3$ was important in the generation of itch via DRG sensory neurons, with signal propagation involving the TRPV1 and TRPA1 channels and the neuropeptide NPPB. Next, we confirmed that keratinocytes secreted periostin in response to the cytokine TSLP via the JAK/STAT pathway. We finally reported the release of periostin in the skin of two mouse models of allergic skin disease and that this allergic itch depended on the β3 integrin. Overall, we report that periostin-induced activation of the $\alpha_V\beta3$ integrin in DRG sensory neurons, and we propose the involvement of a TSLP-periostin reciprocal amplification loop that links the skin to sensory neurons to cause chronic allergic itch.

The Periostin-Induced Itch Is Mediated through Sensory Neurons

AD is often triggered by exposure to allergens that leads to chronic, often severe, cutaneous inflammation and its associated itch. An array of mediators has been shown to be involved in the various facets of cutaneous inflammation and the allergic itch response (Cevikbas et al., 2014; Cianferoni and Spergel, 2014; Indra, 2013; Liu et al., 2016; Masuoka et al., 2012; Oetjen et al., 2017; Shang et al., 2016; Wilson et al., 2013). The fasciclin periostin is one of these chronic inflammatory mediators, but its direct stimulation of sensory neurons and its involvement in the induction of itch had not been reported earlier. Periostin, generally classified as an ECM protein, is produced by several cell types, including epithelial cells and fibroblasts (Masuoka et al., 2012; Rosselli-Murai et al., 2013). It has been suggested that immune cells and parenchymal stromal cells are activated by periostin and participate in the genesis of AD skin lesions (Kim et al., 2017; Masuoka et al., 2012; Uchida et al., 2012). Periostin is highly expressed in the skin of human patients—and dogs—with spontaneous AD (Arima et al., 2015; Izuhara et al., 2014, 2017; Kou et al., 2014; Masuoka et al., 2012; Mineshige et al., 2018; Murota et al., 2017; Yamaguchi, 2014). Our results using immunodeficient mice suggest that periostin directly activates sensory neurons; however, the indirect activation of other cells types (e.g., keratinocytes, fibroblasts, and dendritic cells) by periostin remains possible and needs to be investigated using sophisticated genetic strategies in mice. In humans, serum levels of periostin correlate with the severity and chronicity of AD skin lesions (Kou et al., 2014). Herein, we showed that periostin induced itch behaviors in mice, dogs, and monkeys, which suggests a direct relevance of this cytokine not only in the generation of skin lesions but also in that of itch.

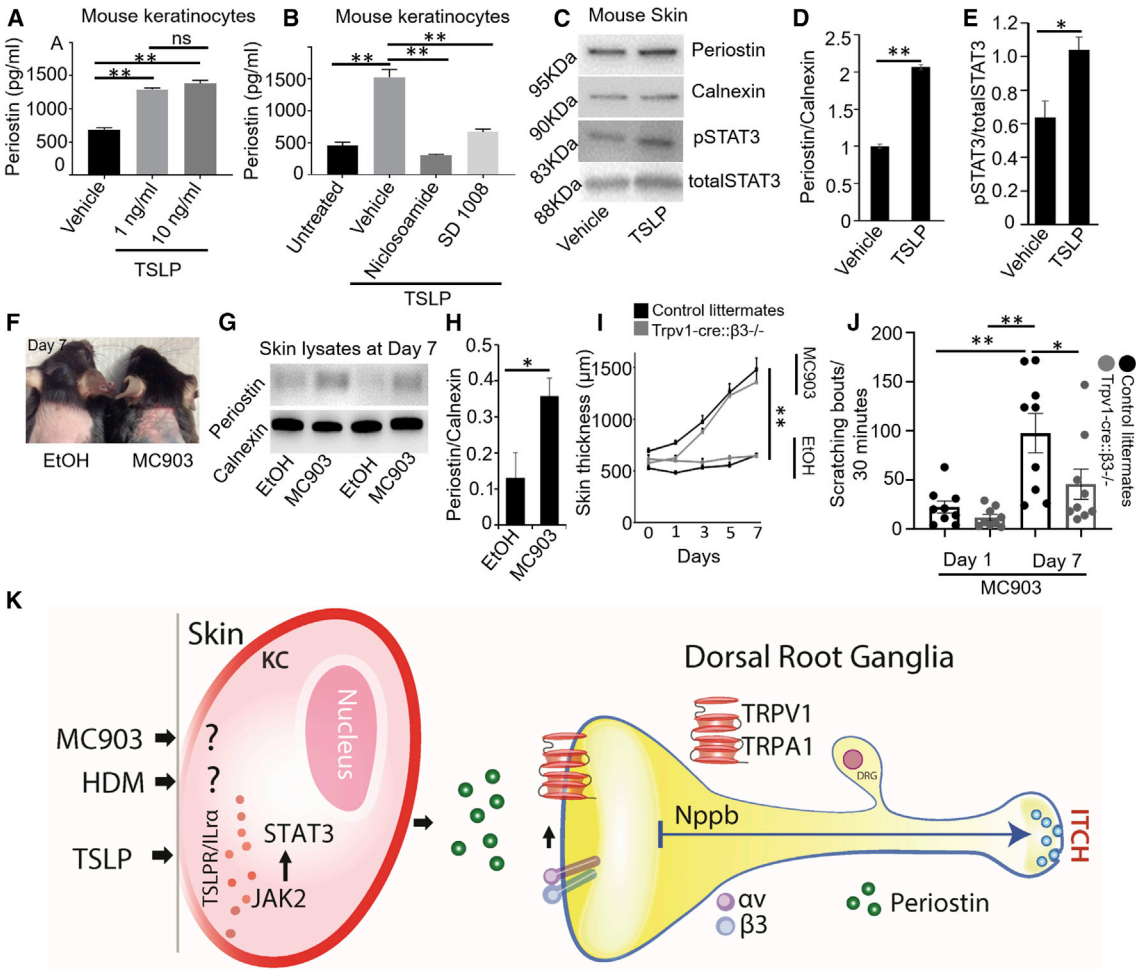

Figure 7. Keratinocytes Secrete Periostin in Response to TSLP Stimulus and the Activation of the JAK/STAT Pathway

(A) TSLP provoked the release of periostin from BALB/MK2 mouse keratinocytes. Equal numbers of cells (50,000 cells/well) were plated and treated with 1 and 10 ng/mL of TSLP, and supernatants were analyzed after 24 h by ELISA. n = 3 independent treatments at each concentration.

(B) Inhibitory effect of the JAK2 inhibitor SD 1008 and the STAT3 inhibitor niclosamide on TSLP-induced periostin production and release by mouse BALB/MK2 keratinocytes. Cells were pre-treated for 4 h with SD 1008 or niclosamide, and then stimulated with 10 ng/mL of TSLP and periostin release measured by ELISA after 24 h. n = 3 independent treatments at each concentration.

(C) Representative immunoblots of periostin and pSTAT3 showed that both were upregulated in mouse skin in response to TSLP (10 ng/mL) compared with vehicle (PBS) treatment. Samples were probed with antibodies against periostin, calnexin, pSTAT3, and total STAT3.

(D) Quantification of periostin normalized with calnexin. n = 3 mice

(E) Quantification of pSTAT3 normalized with total STAT3. n = 3 mice.

(F) Topical application of vehicle (ethanol, left mouse) and 4 nmol of vitamin D analog calcipotriol (MC903, right mouse) each day up to 7 days. MC903 induced erythema and scaling compared with ethanol-treated mice. The picture was taken on day 7.

(G) Representative immunoblot of periostin and calnexin as a control were performed using skin lysates of vehicle- and MC903-treated mice on day 7. MC903 (4 nmol) and ethanol were applied onto the neck of C57BL/6 mice.

(H) Quantification of periostin normalized with calnexin led to a significant increase in periostin production in mice treated with MC903 compared with ethanol. n = 4 mice.

(I) Skin thickness was measured on each day. MC903 induced skin thickness compared with vehicle-treated mice, but no change was seen in skin thickness between control (black) and TRPV1-cre::$\beta3^{-/-}$ (gray) littermates. n = 4–5 mice.

(J) MC903-induced scratching bouts were day dependent and significantly increased at day 7 when compared with day 1. TRPV1-cre::$\beta3^{-/-}$ (gray) littermates showed a significant reduction in scratching bouts compared with control littermates (black). n = 9 mice.

(K) TSLP, MC903, and HDMs induce the release of periostin in the skin. The secreted periostin then binds to the integrin receptor $\alpha_V\beta3$ on DRG sensory neurons, activates downstream TRP channels (TRPV1 and TRPA1) to later release the neurotransmitters/neuropeptides NPPB in the spinal cord, and activates one or more interneurons to eventually induce itch.

All data in (A)–(J) were presented as mean ± SEM. One-way and two-way ANOVA Dunn's tests were performed as appropriate (*p ≤ 0.05, **p ≤ 0.01), and Student's t test was performed between two groups (*p ≤ 0.05, **p ≤ 0.01).

Periostin Activates the Integrin $\alpha_V\beta3$ on Sensory Neurons

Integrins are transmembrane receptors that mediate the adhesion between adjacent cells and/or the ECM. Integrins have diverse roles in several biological processes, including cell migration, development, wound healing, cell differentiation, and apoptosis (Ghatak et al., 2016; Lee and Juliano, 2004). Each integrin exists as a heterodimer consisting of an α subunit and a β subunit (Hynes, 2002). Many painful conditions have been associated with alterations in the ECM. Furthermore, integrins are present on sensory neurons that mediate inflammatory and neuropathic pain (Dina et al., 2004). The fibronectin/integrin pair participates in the upregulation of P2X4 expression after nerve injury and its subsequent neuropathic pain (Tsuda et al., 2008). The upregulation of the integrin $\beta1$ subunit in small- and medium-diameter neurons contributes to substance P-mediated pain after mechanical injury of the capsular ligament (Zhang et al., 2017). The role of integrins in the propagation of itch and how integrins activate neuronal excitability in the DRG sensory neurons have not been reported.

Our study has provided insights into the sensory biology of itch mediated via the integrin $\alpha_V\beta3$. Thus, we speculate on the role of integrin $\alpha_V\beta3$-mediated neuronal excitability through TRP channels via two possible pathways. First, the binding of the ligand periostin to the integrin leads to neuronal signal transduction through the Src kinase, which phosphorylates the TRP channels TRPV1 and TRPA1 and causes an influx of calcium that leads to the enhanced excitability of the sensory neurons and itch induction. A second hypothesis is that integrin and TRP channels are in physical contact with each other and that the activation of the integrin directly leads to TRP channel activation. Further research will be important to understand the neuronal mechanisms that lead to itch mediated through the interaction between integrin $\alpha_V\beta3$ and TRP channels.

Surprisingly, we found that another receptor for periostin, the integrin $\alpha_V\beta5$, was also expressed by almost all DRG neurons, but its role in sensory processing is still unclear and deserves further investigation. We believe this integrin was not relevant in itch transduction, because it appears to be expressed on all DRG neurons, whereas itch-transmitting sensory neurons are a small fraction of these DRG neurons. It is conceivable that the integrin $\alpha_V\beta5$ could play a role in cell adhesion and signaling, while $\alpha_V\beta3$ would be involved in the generation of neuronal excitability via TRP channels. The exact role of these various integrin subunits needs to be explored in the future using mice with neuron-specific deletions of single subunits. Similarly, the integrins $\alpha_V\beta3$ and $\alpha_V\beta5$ are expressed in keratinocytes, but the presence of functional TRPV1 and TRPA1 in these epithelial cells is the subject of controversy. Although some studies support the presence of the TRPV1 and TRPA1 ion channels in keratinocytes (Ho and Lee, 2015), several other reports suggest their absence from mouse keratinocytes (Chung et al., 2003, 2004; Zappia et al., 2016). Further studies using keratinocyte-specific integrin-deficient mice are essential to resolve the role of keratinocytes in the periostin-associated itch in AD. Altogether, our findings suggest the role of the integrin $\alpha_V\beta3$ in itch, which could be used as a potential therapeutic target in the treatment of itch associated with AD.

The Integrin $\alpha_V\beta3$ Uses TRP Channels and the Neuropeptide NPPB to Transmit Periostin-Induced Itch

Both TRPV1 and TRPA1 are generally required for the transmission of itch and pain stimuli to the CNS in rodents (Basbaum et al., 2009; Bautista et al., 2013; Julius, 2013; Julius and Basbaum, 2001; Wilson et al., 2011). Studies have shown that the pro-allergic cytokine TSLP induces itch via the activation of TRPA1 (Wilson et al., 2013). Another Th2 cytokine involved in the AD-associated itch, IL-31, leads to activation of both TRPV1 and TRPA1 (Cevikbas et al., 2014). We herein demonstrated that the ECM protein periostin, which is also relevant in the pathogenesis of chronic AD, activates both TRPV1 and TRPA1 downstream of its $\alpha_V\beta3$ receptor, as shown for IL-31. Herein, we found an overlap between neurons responsive to periostin and those responsive to the two other pruritogenic cytokines: IL-31 and TSLP. Altogether, this potential overlap between the endogenous AD-relevant mediators suggests that these three cytokines might act synergistically to lead to and then perpetuate chronic allergic itch.

The neurotransmitter NPPB has been shown to be relevant for the mechanism of IL-31-associated and chemical-induced itch (Mishra and Hoon, 2013; Pitake et al., 2018). We showed herein that the binding of periostin to the integrin $\alpha_V\beta3$ is mediated via a TRPV1- and TRPA1-induced neuronal depolarization that results in the release of NPPB. A recent report shows that TRPA1 is not co-localized with NPPB-expressing neurons in the DRG (Nguyen et al., 2017), which suggests the existence of a parallel release of other neurotransmitters/neuropeptides in the DRG in response to peripheral pruritogens. After release, NPPB binds to its receptor NPRA on spinal cord interneurons, which in turn depolarizes and releases gastrin-releasing peptide (GRP) to activate gastrin-releasing peptide receptor (GRPR)-expressing interneurons before sending an itch signal to the brain (Mishra and Hoon, 2013). Our behavioral results implicate NPPB in the periostin-mediated itch. Although NPPB plays an important role in signaling between the DRG and the spinal cord, such signaling does not exclude the involvement of other potential neurotransmitters linked to TRPA1 channels.

The Secretion of Periostin Is Regulated by the TSLP Activation of the TSLPR/JAK/STAT Pathway in Keratinocytes

Several molecular responses could lead to chronic itch. The first point of contact between the skin and the external/internal stimuli is the epidermis, which is made up mostly of keratinocytes. Pro-allergic stimuli activate keratinocytes to release the cytokine TSLP, a cytokine known to be involved in allergic itch, AD, asthma, and other inflammatory conditions (Cianferoni and Spergel, 2014; Indra, 2013; Straumann et al., 2001; West et al., 2012; Wilson et al., 2013). The released TSLP could then bind back to keratinocytes via an autocrine/paracrine mechanism involving the TSLPR to induce the secretion periostin via the JAK/STAT3 pathway. Could a vicious circle involving the reciprocal activation of the pruritogenic cytokines TSLP and periostin be one of the explanations for the chronic itch of AD? Previous studies have shown that the archetypal Th2 cytokines IL-4 and IL-13, which are uniquely important to the pathogenesis of AD, stimulate dermal fibroblasts to produce periostin and that such

cytokines activate integrin-expressing keratinocytes to produce TSLP (Izuhara et al., 2014; Masuoka et al., 2012). Herein, we show that TSLP also activates TSLPR-expressing keratinocytes to secrete periostin. Thus, we hypothesize that the cytokines activate each other's secretion by keratinocytes, likely causing a reciprocal amplification loop that results in more of each cytokine being produced over time. Importantly, a vicious circle of amplification such as this might occur without the need for any external factor, such as AD-inducing allergens. Both TSLP (Wilson et al., 2013) and periostin (our work) are now shown to induce itch by directly stimulating DRG sensory neurons. TSLP, MC903, and HDMs all lead to an increase in the secretion of periostin that could, hypothetically, result in the paracrine release of more TSLP, resulting in the continuous stimulation of itch-sensing DRG neurons to induce an ever-worsening itch (Figure 7K). This cutaneous-neuronal interaction could be one of the pathways involved in the chronic and often severe allergic itch that is typical of AD in humans and dogs. The existence of a putative TSLP-periostin inflammation and itch-promoting reciprocal amplification loop unveils the opportunity for therapeutic interventions attempting to block this vicious cycle. Because the anti-TSLP monoclonal antibody tezepelumab proved to have only modest effects in treating the skin lesions of itch of human AD (Simpson et al., 2017), interventions targeting periostin or its integrin receptor might be alternatives worth exploring to treat atopic itch.

STAR★METHODS

Detailed methods are provided in the online version of this paper and include the following:

- KEY RESOURCES TABLE
- RESOURCE AVAILABILITY
  - Lead contact
  - Materials availability
  - Data and code availability
- EXPERIMENTAL MODEL AND SUBJECT DETAILS
  - Animals
- METHOD DETAILS
  - Itch and pain behavioral measurements
  - Allergic model to quantify chronic itch and periostin
  - DRG cell culture
  - Mast cell release and degranulation
  - Calcium imaging on mast cells
  - Immunohistochemistry
  - Quantification of periostin from mouse cell line
  - Calcium imaging on mouse DRG neurons
  - Whole-cell patch clamp recordings in DRG neurons
  - Reverse Transcription-PCR
  - Western blot (WB)
- QUANTIFICATION AND STATISTICAL ANALYSIS

SUPPLEMENTAL INFORMATION

Supplemental Information can be found online at https://doi.org/10.1016/j.celrep.2020.03.036.

ACKNOWLEDGMENTS

We thank Marcelo Rodriguez for providing the BALB/MK2 keratinocyte cell line, Dr. Joy Rachel Ganchingco for demonstrating the isolation of dog DRG neurons, and Ms. Sayee Shruthi Manickam for helping with the assessment of the calcipotriol-related mouse itch behavior. In addition, we thank Ms. Alice Harvey for helping with the illustrations. This study was supported by NC State/CVM startup funds to S.K.M. The NHP study is supported by grant AR-064456 to M.C.K. A private gift provided by Dr. John M. Davis supported a graduate scholarship for J.J.W.

AUTHOR CONTRIBUTIONS

S.K.M. and T.O. conceived the project. S.K.M. designed the experiments and supervised their completion. S.K.M., J.J.W., S.P., H.D., C.J., T.F., J.S.P., P.R., J.C., J.D., L.C.E.-H., M.P., G.P.C., W.B., R.-R.J., M.-C.K., and T.O. performed the experiments and/or analyzed the data. S.K.M. and T.O. wrote the manuscript, with later input from all authors.

DECLARATION OF INTERESTS

The authors declare no competing interests.

Received: May 27, 2019
Revised: February 4, 2020
Accepted: March 11, 2020
Published: April 7, 2020

REFERENCES

Abuabara, K., Yu, A.M., Okhovat, J.P., Allen, I.E., and Langan, S.M. (2018). The prevalence of atopic dermatitis beyond childhood: A systematic review and meta-analysis of longitudinal studies. Allergy *73*, 696–704.

Adamson, A.S. (2017). The Economics Burden of Atopic Dermatitis. Adv. Exp. Med. Biol. *1027*, 79–92.

Arima, K., Ohta, S., Takagi, A., Shiraishi, H., Masuoka, M., Ontsuka, K., Suto, H., Suzuki, S., Yamamoto, K., Ogawa, M., et al. (2015). Periostin contributes to epidermal hyperplasia in psoriasis common to atopic dermatitis. Allergol. Int. *64*, 41–48.

Basbaum, A.I., Bautista, D.M., Scherrer, G., and Julius, D. (2009). Cellular and molecular mechanisms of pain. Cell *139*, 267–284.

Bautista, D.M., Pellegrino, M., and Tsunozaki, M. (2013). TRPA1: A gatekeeper for inflammation. Annu. Rev. Physiol. *75*, 181–200.

Bautista, D.M., Wilson, S.R., and Hoon, M.A. (2014). Why we scratch an itch: the molecules, cells and circuits of itch. Nat. Neurosci. *17*, 175–182.

Bosma, G.C., Custer, R.P., and Bosma, M.J. (1983). A severe combined immunodeficiency mutation in the mouse. Nature *301*, 527–530.

Brenner, D.S., Golden, J.P., and Gereau, R.W., 4th. (2012). A novel behavioral assay for measuring cold sensation in mice. PLoS ONE *7*, e39765.

Carstens, E. (2008). Scratching the brain to understand neuropathic itch. J. Pain *9*, 973–974.

Cevikbas, F., Wang, X., Akiyama, T., Kempkes, C., Savinko, T., Antal, A., Kukova, G., Buhl, T., Ikoma, A., Buddenkotte, J., et al. (2014). A sensory neuron-expressed IL-31 receptor mediates T helper cell-dependent itch: Involvement of TRPV1 and TRPA1. J. Allergy Clin. Immunol. *133*, 448–460.

Chung, M.K., Lee, H., and Caterina, M.J. (2003). Warm temperatures activate TRPV4 in mouse 308 keratinocytes. J. Biol. Chem. *278*, 32037–32046.

Chung, M.K., Lee, H., Mizuno, A., Suzuki, M., and Caterina, M.J. (2004). TRPV3 and TRPV4 mediate warmth-evoked currents in primary mouse keratinocytes. J. Biol. Chem. *279*, 21569–21575.

Cianferoni, A., and Spergel, J. (2014). The importance of TSLP in allergic disease and its role as a potential therapeutic target. Expert Rev. Clin. Immunol. *10*, 1463–1474.

Cruse, G., Beaven, M.A., Ashmole, I., Bradding, P., Gilfillan, A.M., and Metcalfe, D.D. (2013). A truncated splice-variant of the FcεRIβ receptor subunit is critical for microtubule formation and degranulation in mast cells. Immunity *38*, 906–917.

Dillon, S.R., Sprecher, C., Hammond, A., Bilsborough, J., Rosenfeld-Franklin, M., Presnell, S.R., Haugen, H.S., Maurer, M., Harder, B., Johnston, J., et al. (2004). Interleukin 31, a cytokine produced by activated T cells, induces dermatitis in mice. Nat. Immunol. *5*, 752–760.

Dina, O.A., Parada, C.A., Yeh, J., Chen, X., McCarter, G.C., and Levine, J.D. (2004). Integrin signaling in inflammatory and neuropathic pain in the rat. Eur. J. Neurosci. *19*, 634–642.

Eckert, L., Gupta, S., Amand, C., Gadkari, A., Mahajan, P., and Gelfand, J.M. (2017). Impact of atopic dermatitis on health-related quality of life and productivity in adults in the United States: An analysis using the National Health and Wellness Survey. J. Am. Acad. Dermatol. *77*, 274–279.

Eckert, L., Gupta, S., Amand, C., Gadkari, A., Mahajan, P., and Gelfand, J.M. (2018).). The burden of atopic dermatitis in US adults: Health care resource utilization data from the 2013 National Health and Wellness Survey. J. Am. Acad. Dermatol. *78*, 54–61.

Fukuyama, T., Ehling, S., Cook, E., and Bäumer, W. (2015). Topically Administered Janus-Kinase Inhibitors Tofacitinib and Oclacitinib Display Impressive Antipruritic and Anti-Inflammatory Responses in a Model of Allergic Dermatitis. J. Pharmacol. Exp. Ther. *354*, 394–405.

Fukuyama, T., Martel, B.C., Linder, K.E., Ehling, S., Ganchingco, J.R., and Bäumer, W. (2018). Hypochlorous acid is antipruritic and anti-inflammatory in a mouse model of atopic dermatitis. Clin. Exp. Allergy *48*, 78–88.

Ghatak, S., Niland, S., Schulz, J.N., Wang, F., Eble, J.A., Leitges, M., Mauch, C., Krieg, T., Zigrino, P., and Eckes, B. (2016). Role of Integrins α1β1 and α2β1 in Wound and Tumor Angiogenesis in Mice. Am. J. Pathol. *186*, 3011–3027.

Gillan, L., Matei, D., Fishman, D.A., Gerbin, C.S., Karlan, B.Y., and Chang, D.D. (2002). Periostin secreted by epithelial ovarian carcinoma is a ligand for alpha(V)beta(3) and alpha(V)beta(5) integrins and promotes cell motility. Cancer Res. *62*, 5358–5364.

Goodman, S.L., Hölzemann, G., Sulyok, G.A., and Kessler, H. (2002). Nanomolar small molecule inhibitors for alphav(beta)6, alphav(beta)5, and alphav(beta)3 integrins. J. Med. Chem. *45*, 1045–1051.

Grimbaldeston, M.A., Chen, C.C., Piliponsky, A.M., Tsai, M., Tam, S.Y., and Galli, S.J. (2005). Mast cell-deficient W-sash c-kit mutant Kit W-sh/W-sh mice as a model for investigating mast cell biology *in vivo*. Am. J. Pathol. *167*, 835–848.

Han, L., and Dong, X. (2014). Itch mechanisms and circuits. Annu. Rev. Biophys. *43*, 331–355.

Han, S.K., Mancino, V., and Simon, M.I. (2006). Phospholipase Cbeta 3 mediates the scratching response activated by the histamine H1 receptor on C-fiber nociceptive neurons. Neuron *52*, 691–703.

Han, L., Ma, C., Liu, Q., Weng, H.J., Cui, Y., Tang, Z., Kim, Y., Nie, H., Qu, L., Patel, K.N., et al. (2013). A subpopulation of nociceptors specifically linked to itch. Nat. Neurosci. *16*, 174–182.

Han, Q., Liu, D., Convertino, M., Wang, Z., Jiang, C., Kim, Y.H., Luo, X., Zhang, X., Nackley, A., Dokholyan, N.V., and Ji, R.R. (2018). miRNA-711 Binds and Activates TRPA1 Extracellularly to Evoke Acute and Chronic Pruritus. Neuron *99*, 449–463.

Hermanns, H.M. (2015). Oncostatin M and interleukin-31: Cytokines, receptors, signal transduction and physiology. Cytokine Growth Factor Rev. *26*, 545–558.

Ho, J.C., and Lee, C.H. (2015). TRP channels in skin: from physiological implications to clinical significances. Biophysics (Nagoya-shi) *11*, 17–24.

Huang, J., Polgár, E., Solinski, H.J., Mishra, S.K., Tseng, P.Y., Iwagaki, N., Boyle, K.A., Dickie, A.C., Kriegbaum, M.C., Wildner, H., et al. (2018). Circuit dissection of the role of somatostatin in itch and pain. Nat. Neurosci. *21*, 707–716.

Hynes, R.O. (2002). Integrins: bidirectional, allosteric signaling machines. Cell *110*, 673–687.

Imamachi, N., Park, G.H., Lee, H., Anderson, D.J., Simon, M.I., Basbaum, A.I., and Han, S.K. (2009). TRPV1-expressing primary afferents generate behavioral responses to pruritogens via multiple mechanisms. Proc. Natl. Acad. Sci. USA *106*, 11330–11335.

Indra, A.K. (2013). Epidermal TSLP: a trigger factor for pathogenesis of atopic dermatitis. Expert Rev. Proteomics *10*, 309–311.

Izuhara, K., Arima, K., Ohta, S., Suzuki, S., Inamitsu, M., and Yamamoto, K.I. (2014). Periostin in Allergic Inflammation. Allergol. Int. *63*, 143–151.

Izuhara, K., Nunomura, S., Nanri, Y., Ogawa, M., Ono, J., Mitamura, Y., and Yoshihara, T. (2017). Periostin in inflammation and allergy. Cell. Mol. Life Sci. *74*, 4293–4303.

Jensen, B.M., Swindle, E.J., Iwaki, S., and Gilfillan, A.M. (2006). Generation, isolation, and maintenance of rodent mast cells and mast cell lines. Curr. Protoc. Immunol. *74*, 3.23.1–3.23.13.

Julius, D. (2013). TRP channels and pain. Annu. Rev. Cell Dev. Biol. *29*, 355–384.

Julius, D., and Basbaum, A.I. (2001). Molecular mechanisms of nociception. Nature *413*, 203–210.

Kardon, A.P., Polgár, E., Hachisuka, J., Snyder, L.M., Cameron, D., Savage, S., Cai, X., Karnup, S., Fan, C.R., Hemenway, G.M., et al. (2014). Dynorphin acts as a neuromodulator to inhibit itch in the dorsal horn of the spinal cord. Neuron *82*, 573–586.

Kim, D.W., Kulka, M., Jo, A., Eun, K.M., Arizmendi, N., Tancowny, B.P., Hong, S.N., Lee, J.P., Jin, H.R., Lockey, R.F., et al. (2017). Cross-Talk Between Human Mast Cells and Epithelial Cells By IgE-Mediated Periostin Production in Eosinophilic Nasal Polyps. J. Allergy Clin. Immunol. *139*, 1692–1695.

Kittaka, H., and Tominaga, M. (2017). The molecular and cellular mechanisms of itch and the involvement of TRP channels in the peripheral sensory nervous system and skin. Allergol. Int. *66*, 22–30.

Ko, M.C., and Naughton, N.N. (2000). An experimental itch model in monkeys: characterization of intrathecal morphine-induced scratching and antinociception. Anesthesiology *92*, 795–805.

Kou, K., Okawa, T., Yamaguchi, Y., Ono, J., Inoue, Y., Kohno, M., Matsukura, S., Kambara, T., Ohta, S., Izuhara, K., and Aihara, M. (2014). Periostin levels correlate with disease severity and chronicity in patients with atopic dermatitis. Br. J. Dermatol. *171*, 283–291.

Lagerström, M.C., Rogoz, K., Abrahamsen, B., Persson, E., Reinius, B., Nordenankar, K., Olund, C., Smith, C., Mendez, J.A., Chen, Z.F., et al. (2010). VGLUT2-dependent sensory neurons in the TRPV1 population regulate pain and itch. Neuron *68*, 529–542.

Lee, J.W., and Juliano, R. (2004). Mitogenic signal transduction by integrin- and growth factor receptor-mediated pathways. Mol. Cells *17*, 188–202.

Li, G., Jin, R., Norris, R.A., Zhang, L., Yu, S., Wu, F., Markwald, R.R., Nanda, A., Conway, S.J., Smyth, S.S., and Granger, D.N. (2010). Periostin mediates vascular smooth muscle cell migration through the integrins alphavbeta3 and alphavbeta5 and focal adhesion kinase (FAK) pathway. Atherosclerosis *208*, 358–365.

Liu, T., and Ji, R.R. (2014). Toll-Like Receptors and Itch. In Itch: Mechanisms and Treatment, E. Carstens and T. Akiyama, eds. (CRC Press/Taylor & Francis).

Liu, B., Tai, Y., Achanta, S., Kaelberer, M.M., Caceres, A.I., Shao, X., Fang, J., and Jordt, S.E. (2016). IL-33/ST2 signaling excites sensory neurons and mediates itch response in a mouse model of poison ivy contact allergy. Proc. Natl. Acad. Sci. USA *113*, E7572–E7579.

Ma, Q. (2014). Itch Modulation by VGLUT2-Dependent Glutamate Release from Somatic Sensory Neurons. In Itch: Mechanisms and Treatment, E. Carstens and T. Akiyama, eds. (CRC Press/Taylor & Francis).

Madisen, L., Zwingman, T.A., Sunkin, S.M., Oh, S.W., Zariwala, H.A., Gu, H., Ng, L.L., Palmiter, R.D., Hawrylycz, M.J., Jones, A.R., et al. (2010). A robust and high-throughput Cre reporting and characterization system for the whole mouse brain. Nat. Neurosci. *13*, 133–140.

Masuoka, M., Shiraishi, H., Ohta, S., Suzuki, S., Arima, K., Aoki, S., Toda, S., Inagaki, N., Kurihara, Y., Hayashida, S., et al. (2012). Periostin promotes

chronic allergic inflammation in response to Th2 cytokines. J. Clin. Invest. *122*, 2590–2600.

Merryman-Simpson, A.E., Wood, S.H., Fretwell, N., Jones, P.G., McLaren, W.M., McEwan, N.A., Clements, D.N., Carter, S.D., Ollier, W.E., and Nuttall, T. (2008). Gene (mRNA) expression in canine atopic dermatitis: microarray analysis. Vet. Dermatol. *19*, 59–66.

Mineshige, T., Kamiie, J., Sugahara, G., Yasuno, K., Aihara, N., Kawarai, S., Yamagishi, K., Shirota, M., and Shirota, K. (2015). Expression of Periostin in Normal, Atopic, and Nonatopic Chronically Inflamed Canine Skin. Vet. Pathol. *52*, 1118–1126.

Mineshige, T., Kamiie, J., Sugahara, G., and Shirota, K. (2018). A study on periostin involvement in the pathophysiology of canine atopic skin. J. Vet. Med. Sci. *80*, 103–111.

Mishra, S.K., and Hoon, M.A. (2010). Ablation of TrpV1 neurons reveals their selective role in thermal pain sensation. Mol. Cell. Neurosci. *43*, 157–163.

Mishra, S.K., and Hoon, M.A. (2013). The cells and circuitry for itch responses in mice. Science *340*, 968–971.

Mishra, S.K., and Hoon, M.A. (2015). Transmission of pruriceptive signals. Handb. Exp. Pharmacol. *226*, 151–162.

Mishra, S.K., Tisel, S.M., Orestes, P., Bhangoo, S.K., and Hoon, M.A. (2011). TRPV1-lineage neurons are required for thermal sensation. EMBO J. *30*, 582–593.

Mollanazar, N.K., Smith, P.K., and Yosipovitch, G. (2016). Mediators of Chronic Pruritus in Atopic Dermatitis: Getting the Itch Out? Clin. Rev. Allergy Immunol. *51*, 263–292.

Mombaerts, P., Iacomini, J., Johnson, R.S., Herrup, K., Tonegawa, S., and Papaioannou, V.E. (1992). RAG-1-deficient mice have no mature B and T lymphocytes. Cell *68*, 869–877.

Moosbrugger-Martinz, V., Schmuth, M., and Dubrac, S. (2017). A Mouse Model for Atopic Dermatitis Using Topical Application of Vitamin D3 or of Its Analog MC903. Methods Mol. Biol. *1559*, 91–106.

Morgan, E.A., Schneider, J.G., Baroni, T.E., Uluçkan, O., Heller, E., Hurchla, M.A., Deng, H., Floyd, D., Berdy, A., Prior, J.L., et al. (2010). Dissection of platelet and myeloid cell defects by conditional targeting of the beta3-integrin subunit. FASEB J. *24*, 1117–1127.

Murota, H., Lingli, Y., and Katayama, I. (2017). Periostin in the pathogenesis of skin diseases. Cell. Mol. Life Sci. *74*, 4321–4328.

Nguyen, M.Q., Wu, Y., Bonilla, L.S., von Buchholtz, L.J., and Ryba, N.J.P. (2017). Diversity amongst trigeminal neurons revealed by high throughput single cell sequencing. PLoS ONE *12*, e0185543.

Oaklander, A.L. (2011). Neuropathic itch. Semin. Cutan. Med. Surg. *30*, 87–92.

Odhiambo, J.A., Williams, H.C., Clayton, T.O., Robertson, C.F., and Asher, M.I.; ISAAC Phase Three Study Group (2009). Global variations in prevalence of eczema symptoms in children from ISAAC Phase Three. J. Allergy Clin. Immunol. *124*, 1251–1258.

Oetjen, L.K., Mack, M.R., Feng, J., Whelan, T.M., Niu, H., Guo, C.J., Chen, S., Trier, A.M., Xu, A.Z., Tripathi, S.V., et al. (2017). Sensory Neurons Co-opt Classical Immune Signaling Pathways to Mediate Chronic Itch. Cell *171*, 217–228.

Olivry, T., and Bäumer, W. (2015). Atopic itch in dogs: pharmacology and modeling. Handb. Exp. Pharmacol. *226*, 357–369.

Olivry, T., Mayhew, D., Paps, J.S., Linder, K.E., Peredo, C., Rajpal, D., Hofland, H., and Cote-Sierra, J. (2016). Early Activation of Th2/Th22 Inflammatory and Pruritogenic Pathways in Acute Canine Atopic Dermatitis Skin Lesions. J. Invest. Dermatol. *136*, 1961–1969.

Paps, J.S., Bäumer, W., and Olivry, T. (2016). Development of an Allergen-induced Atopic Itch Model in Dogs: A Preliminary Report. Acta Derm. Venereol. *96*, 400–401.

Park, K., Park, J.H., Yang, W.J., Lee, J.J., Song, M.J., and Kim, H.P. (2012). Transcriptional activation of the IL31 gene by NFAT and STAT6. J. Leukoc. Biol. *91*, 245–257.

Paus, R., Schmelz, M., Bíró, T., and Steinhoff, M. (2006). Frontiers in pruritus research: scratching the brain for more effective itch therapy. J. Clin. Invest. *116*, 1174–1186.

Pitake, S., Ralph, P.C., DeBrecht, J., and Mishra, S.K. (2018). Atopic Dermatitis Linked Cytokine Interleukin-31 Induced Itch Mediated via a Neuropeptide Natriuretic Polypeptide B. Acta Derm. Venereol. *98*, 795–796.

Pogorzala, L.A., Mishra, S.K., and Hoon, M.A. (2013). The cellular code for mammalian thermosensation. J. Neurosci. *33*, 5533–5541.

Rosselli-Murai, L.K., Almeida, L.O., Zagni, C., Galindo-Moreno, P., Padial-Molina, M., Volk, S.L., Murai, M.J., Rios, H.F., Squarize, C.H., and Castilho, R.M. (2013). Periostin responds to mechanical stress and tension by activating the MTOR signaling pathway. . PLoS One *8*, e83580.

Ruan, K., Bao, S., and Ouyang, G. (2009). The multifaceted role of periostin in tumorigenesis. Cell. Mol. Life Sci. *66*, 2219–2230.

Shahwan, K.T., and Kimball, A.B. (2017).). Itch intensity in moderate-to-severe plaque psoriasis versus atopic dermatitis: A meta-analysis. J. Am. Acad. Dermatol. *76*, 1198–1200.

Shang, H., Cao, X.L., Wan, Y.J., Meng, J., and Guo, L.H. (2016). IL-4 Gene Polymorphism May Contribute to an Increased Risk of Atopic Dermatitis in Children. . Dis. Markers *2016*, 1021942.

Sheahan, T.D., Hachisuka, J., and Ross, S.E. (2018). Small RNAs, but Sizable Itch: TRPA1 Activation by an Extracellular MicroRNA. Neuron *99*, 421–422.

Shim, W.S., Tak, M.H., Lee, M.H., Kim, M., Kim, M., Koo, J.Y., Lee, C.H., Kim, M., and Oh, U. (2007). TRPV1 mediates histamine-induced itching via the activation of phospholipase A2 and 12-lipoxygenase. J. Neurosci. *27*, 2331–2337.

Shimada, S.G., and LaMotte, R.H. (2008). Behavioral differentiation between itch and pain in mouse. Pain *139*, 681–687.

Shiraishi, H., Masuoka, M., Ohta, S., Suzuki, S., Arima, K., Taniguchi, K., Aoki, S., Toda, S., Yoshimoto, T., Inagaki, N., et al. (2012). Periostin contributes to the pathogenesis of atopic dermatitis by inducing TSLP production from keratinocytes. Allergol. Int. *61*, 563–572.

Shultz, L.D., Schweitzer, P.A., Christianson, S.W., Gott, B., Schweitzer, I.B., Tennent, B., McKenna, S., Mobraaten, L., Rajan, T.V., Greiner, D.L., et al. (1995). Multiple defects in innate and adaptive immunologic function in NOD/LtSz-scid mice. J. Immunol. *154*, 180–191.

Simpson, E.L., Bruin-Weller, M., Flohr, C., Ardern-Jones, M.R., Barbarot, S., Deleuran, M., Bieber, T., Vestergaard, C., Brown, S.J., Cork, M.J., et al. (2017). When does atopic dermatitis warrant systemic therapy? Recommendations from an expert panel of the International Eczema Council. J. Am. Acad. Dermatol. *77*, 623–633.

Storan, E.R., O'Gorman, S.M., McDonald, I.D., and Steinhoff, M. (2015). Role of cytokines and chemokines in itch. Handb. Exp. Pharmacol. *226*, 163–176.

Straumann, A., Bauer, M., Fischer, B., Blaser, K., and Simon, H.U. (2001). Idiopathic eosinophilic esophagitis is associated with a T(H)2-type allergic inflammatory response. J. Allergy Clin. Immunol. *108*, 954–961.

Takahashi, N., Sugaya, M., Suga, H., Oka, T., Kawaguchi, M., Miyagaki, T., Fujita, H., and Sato, S. (2016). Thymic Stromal Chemokine TSLP Acts through Th2 Cytokine Production to Induce Cutaneous T-cell Lymphoma. Cancer Res. *76*, 6241–6252.

Tsuda, M., Toyomitsu, E., Komatsu, T., Masuda, T., Kunifusa, E., Nasu-Tada, K., Koizumi, S., Yamamoto, K., Ando, J., and Inoue, K. (2008). Fibronectin/integrin system is involved in P2X(4) receptor upregulation in the spinal cord and neuropathic pain after nerve injury. Glia *56*, 579–585.

Uchida, M., Shiraishi, H., Ohta, S., Arima, K., Taniguchi, K., Suzuki, S., Okamoto, M., Ahlfeld, S.K., Ohshima, K., Kato, S., et al. (2012). Periostin, a matricellular protein, plays a role in the induction of chemokines in pulmonary fibrosis. Am. J. Respir. Cell Mol. Biol. *46*, 677–686.

Usoskin, D., Furlan, A., Islam, S., Abdo, H., Lönnerberg, P., Lou, D., Hjerling-Leffler, J., Haeggström, J., Kharchenko, O., Kharchenko, P.V., et al. (2015). Unbiased classification of sensory neuron types by large-scale single-cell RNA sequencing. Nat. Neurosci. *18*, 145–153.

Voisin, T., Bouvier, A., and Chiu, I.M. (2017). Neuro-immune interactions in allergic diseases: novel targets for therapeutics. Int. Immunol. *29*, 247–261.

Weidinger, S., and Novak, N. (2016). Atopic dermatitis. Lancet *387*, 1109–1122.

West, E.E., Kashyap, M., and Leonard, W.J. (2012). TSLP: A Key Regulator of Asthma Pathogenesis. Drug Discov. Today Dis. Mech. *9*, 003.

Wilson, S.R., Gerhold, K.A., Bifolck-Fisher, A., Liu, Q., Patel, K.N., Dong, X., and Bautista, D.M. (2011). TRPA1 is required for histamine-independent, Mas-related G protein-coupled receptor-mediated itch. Nat. Neurosci. *14*, 595–602.

Wilson, S.R., Thé, L., Batia, L.M., Beattie, K., Katibah, G.E., McClain, S.P., Pellegrino, M., Estandian, D.M., and Bautista, D.M. (2013). The epithelial cell-derived atopic dermatitis cytokine TSLP activates neurons to induce itch. Cell *155*, 285–295.

Yamaguchi, Y. (2014). Periostin in Skin Tissue Skin-Related Diseases. Allergol. Int. *63*, 161–170.

Yosipovitch, G., and Samuel, L.S. (2008). Neuropathic and psychogenic itch. Dermatol. Ther. *21*, 32–41.

Zappia, K.J., Garrison, S.R., Palygin, O., Weyer, A.D., Barabas, M.E., Lawlor, M.W., Staruschenko, A., and Stucky, C.L. (2016). Mechanosensory and ATP Release Deficits following Keratin14-Cre-Mediated TRPA1 Deletion Despite Absence of TRPA1 in Murine Keratinocytes. PLoS ONE *11*, e0151602.

Zhang, S., Zhao, E., and Winkelstein, B.A. (2017). A Nociceptive Role for Integrin Signaling in Pain After Mechanical Injury to the Spinal Facet Capsular Ligament. Ann. Biomed. Eng. *45*, 2813–2825.

STAR★METHODS

KEY RESOURCES TABLE

REAGENT or RESOURCE	SOURCE	IDENTIFIER
Antibodies		
Anti-Calnexin	Sigma Aldrich	C4731; RRID:AB_476845
Anti-STAT6	R&D Systems	AF2167; RRID:AB_355173
Anti-pSTAT6	Sigma Aldrich	SAB 4504546; RRID:AB_2827995
Anti-STAT3	Thermofisher	MA1-13042; RRID:AB_10985240
Anti-pSTAT3	Thermofisher	44-384G; RRID:AB_1502076
Anti-pSTAT5	Sigma Aldrich	SAB4301474; RRID:AB_2827996
Anti-STAT5	Thermofisher	PA5-36075; RRID:AB_1553359
Anti-GAPDH	Santa Cruz Biotechnology	sc-32233; RRID:AB_627679
Anti-Periostin	Thermofisher	PA5-34641; RRID:AB_2551993
Anti-TSLPR	ProSci	4209; RRID:AB_10904285
Anti-ITGB3	Novus Biological	NBP1-60872; RRID:AB_11005987
Goat Anti-Rabbit Cy3	Life Technologies	A10520; RRID:AB_2534029
Goat anti-rabbit IgG-HRP	Santa Cruz Biotechnology	sc-2004; RRID:AB_631746
Goat anti-mouse IgG HRP	Santa Cruz Biotechnology	sc-2005; RRID:AB_631736
Goat Anti-Mouse 488	Life Technologies	A11001; RRID:AB_2534069
Biological Samples		
Mouse DRG	This paper	N/A
Mouse Skin	This paper	N/A
Mast cells	Bone marrow (C57BL6J)	N/A
Chemicals, Peptides, and Recombinant Proteins		
Recombinant Mouse Periostin	R&D Biosystems	Catalog # 2955-F2
Recombinant mouse IL-3	R&D Biosystems	Catalog # 403-ML
Recombinant mouse SCF	R&D Biosystems	Catalog # 455-MC
Mouse anti-DNP IgE (clone SPE-7)	Sigma Aldrich	D8406
DNP-HSA	Sigma Aldrich	A6661
Ionomycin calcium salt	Invitrogen	I24222
Dispase	Fisher Scientific	NC9886504
Collagenase	MP Biomedicals	150704
Laminin	Sigma Aldrich	L2020
DMEM	Atlanta Biologicals	10-013-CV
RPMI-1640	Corning, NY	10-040-CM
Pefabloc	Sigma Aldrich	15633
FBS	Atlanta Biologicals	S11050
PenStrep	VWR	K952
Poly-L-Lysine	Sigma Aldrich	P4704
Fura-2 AM	Enzo	ENZ-52006
Recombinant Mouse TSLP	R&D Biosystems	555-TS
Histamine	Sigma Aldrich	H125
Chloroquine	Sigma Aldrich	C6628
Allyl isothiocyanate (AITC)	Sigma Aldrich	W203408
Capsaicin	Sigma Aldrich	M2028
Cilengitide	Sigma Aldrich	SMC1594
Niclosamide	Tocris Biosciences	4079

(*Continued on next page*)

Continued

REAGENT or RESOURCE	SOURCE	IDENTIFIER
SD 1008	Tocris Biosciences	3035
MC903	Tocris Biosciences	2700
House Dust Mites (*Dermatophagoides farina)*	Greer, Lenoir, NC, USA	NC1563903
Betamethasone dipropionate	Sigma Aldrich	5593
Critical Commercial Assays		
In vivo jetPEI	Polyplus	201-10G
QIAGEN RNEasy Mini Kit	QIAGEN	74704
Mouse Periostin/OSF-2 DuoSet ELISA	R&D Biosystems	DY2955
Experimental Models: Cell Lines		
Mouse Keratinocytes cell line (BALB/MK2 keratinocytes)	This paper	Gift from Dr. Marcelo Rodriguez, CVM/NCSU
Experimental Models: Organisms/Strains		
WT: C57BL/6J	Jackson Labs	Strain Code: 000664
ITGB3$^{fl/fl}$: C57BL/6-Itgb3tm1.1Wlbcr/J	Jackson Labs	Strain Code: 028232
SST-cre: B6J.Cg-Ssttm2.1(cre)Zjh/MwarJ	Jackson Labs	Strain Code: 028864
TRPV1-cre: B6.129-Trpv1tm1(cre)Bbm/J	Jackson Labs	Strain Code: 017769
SST-cre::Ai9	This Paper	Strain Code: N/A
TRPV1-cre::β3−/−	This Paper	Strain Code: N/A
TRPV1 KO: B6.129X1-Trpv1tm1Jul/J	Jackson Labs	Strain Code: 003770
TRPA1 KO: Trpa1tm2.1Kykw/J	Jackson Labs	Strain Code: 008654
TRPV1/A1 Double Knockout	This Paper	Strain Code: N/A
NOD: NOD.CB17-*Prkdc*^{scid}/J	Jackson Labs	Strain Code: 001303
NOD/SCID: NOD/ShiLtJ	Jackson Labs	Strain Code: 001976
Rag1 KO: B6.129S7-*Rag1*^{tm1Mom}/J	Jackson Labs	Strain Code: 002216
Ai9: B6.Cg-*Gt(ROSA)26Sor*$^{tm9(CAG-tdTomato)Hze}$/J	Jackson Labs	Strain Code: 007909
Kit^{W-sh}/HNihrJaeBsmJ	Jackson Labs	005051
NC/Nga	Charles River Lab (Japan)	RBRC01059
Maltese-beagle	in house	CVM/NCSU
Non-Human Primates	in house	Wake Forest School of Medicine
Oligonucleotides		
Taqman Mouse ITGAV Probe Set	Thermofisher	Mm01339538
Taqman Mouse ITGB3 Probe Set	Thermofisher	Mm1240368
Taqman Mouse ITGB5 Probe Set	Thermofisher	Mm00439825
Taqman Mouse ITGA2b Probe Set	Thermofisher	Mm00439747
Taqman Mouse GAPDH Probe Set	Thermofisher	Mm99999615
Taqman Dog ITGAV Probe Set	Thermofisher	Cf02696697
Taqman Dog ITGB3 Probe Set	Thermofisher	Cf02623437
Taqman Dog ITGB5 Probe Set	Thermofisher	Cf02658863
Taqman Dog ITGA2b Probe Set	Thermofisher	Cf02623652
Taqman Dog GAPDH Probe Set	Thermofisher	Cf04419463
Software and Algorithms		
ImageJ	NIH	NA
Prism8	Graphpad	NA
pClamp10 software	Axon Instruments	NA
NIS-Elements AR 5.02.01	Nikon	NA
Other		
Calcium Imaging Scope	Nikon	TE200
Axopatch-700B amplifier	Axon Instrument	N/A

(*Continued on next page*)

Continued

REAGENT or RESOURCE	SOURCE	IDENTIFIER
Eclipse Ti	Nikon, Melville (NY)	N/A
Dynamic Plantar Aesthesiometer	Ugo Basile, Italy	37450
Rotarod Rotomex 5	Columbus Instruments	N/A
Hargreave's Apparatus	Ugo Basile, Italy	N/A
Cold Test	Dry Ice assay	Brenner et al., 2012
BioTek Neo2 multimode plate reader	BioTek	N/A

RESOURCE AVAILABILITY

Lead contact

Further information and requests for resources and reagents should be directed to the lead contact, Santosh K. Mishra (skmishra@ncsu.edu).

Materials availability

There are restrictions to the availability of mouse and cell line generated in this study, due to potential requirements for Materials Transfer Agreement (MTA) with the host institution at which these reagents were generated.

Data and code availability

This study did not generate/analyze DNA or protein datasets.

EXPERIMENTAL MODEL AND SUBJECT DETAILS

Animals

Experiments using animals including mice and dogs (Maltese-beagle), followed the North Carolina State University laboratory animal care protocols approved by an Institutional Animal Care and Use Committee (IACUC) and for non-human primates (NHP) as per NIH guidelines. Mice were housed in small social groups (4 animals) in individually ventilated cages under 12-hour light/dark cycles and fed *ad libitum*. We used 8-12-week old mice both male and females for most of the experiments both in cell cultures as well as in awake animals. For patch clamp studies, cell culture was prepared from female mice. The C57BL/6N and all other genetically modified and knockout (KO) mice (Trpv1-cre; Sst-IRES-Cre; TRPV1 KO; TRPA1 KO; mast cells deficient c-kit mice; B & T cells deficient RAG KO mice and controls; B, T, and NK cells KO mice NOD/SCID and its control NOD) were purchased from the Jackson laboratory (Ellsworth, Maine). TRPV1, TRPA1, and double KO mice were bred in house. Trpv1-IRES-Cre animals were bred to a floxed β3 allele (Morgan et al., 2010), allowing a conditional deletion of β3 in sensory neurons. Sst-IRES-Cre knock-in line was crossed to conditional alleles, to enable the Cre-dependent expression of tdTomato (Ai9) (Madisen et al., 2010) from the R26 locus. Genotyping of offspring from all breeding steps was performed with genomic DNA isolated from tail snips and allele-specific primer pairs.

METHOD DETAILS

Itch and pain behavioral measurements

All behavioral experiments were conducted during the light cycle at ambient temperature (23°C). Behavioral assessment of scratching behavior was conducted as described previously (Mishra et al., 2011). Briefly, mice were injected intradermal into the nape of the neck with periostin (R&D), histamine, and chloroquine (all Millipore-Sigma) as described (Shimada and LaMotte, 2008). Compounds were diluted in PBS and the same was used as a vehicle. For inhibitor study, cilengitide was first injected intradermal (i.d.) to observe any unwanted effect on itch behavior. In separate experiments, cilengitide was injected i.v. and i.p. 10 minutes prior to periostin injection in the dorsal neck. Additionally, we combined cilengitide and periostin together (mix) and injected i.d. into the dorsal neck of mouse. Scratching behavior was recorded for 30 minutes and data was presented in bouts per 30 minutes for mice. One bout was defined as scratching behavior toward the injection site between lifting the hind leg from the ground and either putting it back on the ground or guarding/licking the paw with the mouth. Injections of periostin, and capsaicin in the mouse cheek itch/pain model were performed as described previously (Shimada and LaMotte, 2008). For eye wipes assay, we dropped periostin and capsaicin on mouse cornea and counted wipes for 1-minute. Injection volume was always 20μl in mice. For dog's study, we injected periostin (25μg/25μl) in the dorsal neck (s.c.) and behavior was recorded and quantified for 30 minutes as duration of pruritus manifestation (DPM), as described earlier (Paps et al., 2016). For NHP studies, periostin (25μg/100μl) was injected in the NHP thigh (s.c.) on the lateral side of the upper part of the hind limb; the skin area over the vastus lateralis muscle. The lateral side of the upper part of the hind limb was chosen as an injection site because this location is safe and easy to access when animal is in a chair. The number of scratches is easily countable in NHP. When different raters separately scored a single tape, the ratings indicated high interrater

reliability (coefficient of correlation, r > 0.95). This method of itch readout in NHP has been used and accepted (Ko and Naughton, 2000). The behavior was recorded for 30 minutes duration and number of scratches quantified. In NHP, a scratch is defined as one brief (< 1 s) episode of scraping contact of the forepaw or hind paw on the skin surface

For pain measurement, we conducted experiment as described previously (Mishra and Hoon, 2013; Pogorzala et al., 2013). Mice were acclimatized to plexiglass chambers for 20 minutes and Hargreaves (hot), Dry ice assay (cold), von-Frey (mechanical), and Rotarod (proprioception) were performed on control and mutant mice. Each mouse was recorded twice, and average of each measurements were presented. Experimenters were blind to the genotype or treatment of the mice used in behavioral experiments.

Allergic model to quantify chronic itch and periostin

C57BL6 mice (Jackson Labs) were applied daily with MC903 (4nmol) and vehicle (97% ethanol) after brief anesthesia. Skin thickness was measured using cutimeter as described (Fukuyama et al., 2015). Scratching behavior was video-monitored for 30 min on Day 1 and Day 7. On Day 7 skin was collected from vehicle and MC903 treated mice for the Western Blot (WB) as described below. NC/Nga mice (Charles River, Japan) were sensitized and challenged with house dust mite (HDM) allergen (*Dermatophagoides farina*, Greer, Lenoir, NC, USA as described previously (Fukuyama et al., 2018). In short, for sensitization, 30 μL of HDM in mineral oil (10mg/ml) was applied topically to the clipped back twice weekly supported by tape stripping until visible lesions had developed. After development of visible lesions mice were treated daily either with vehicle cream or betamethasone dipropionate (0.1% in lipoderm, n = 8). Application of betamethasone dipropionate was reduced to every other day on day 26 because of significant weight loss). Scratching behavior was video monitored for 60 min period immediately after HDM on day 42. For periostin measurement, mice were sacrificed for determination of periostin in skin on day 43. A portion of back skin tissue were snap-frozen in liquid nitrogen. Briefly, samples were homogenized under liquid nitrogen, and the homogenates were taken in 200 μL RPMI 1640 medium containing 1 mmol/L Pefabloc. The amount of periostin was determined using ELISA according to the manufacturer's instruction.

DRG cell culture

DRGs were isolated from mice and dissociated in 1ml of media containing 2.5U/ml of dispase (Fisher) and 2.5mg/ml of collagenase (Fisher). After dissociation, the cells were washed with complete media (DMEM (HiMedia) with 10% FBS (Atlanta Biologicals) and 1% PenStrep (VWR)) and pelleted at 1000 rpm for 15 minutes. Approximately 30μl of the cell suspension was plated on 18mm round glass slides with a coating of laminin (Sigma Aldrich) and poly-L-lysine (Sigma Aldrich) and incubated for 1.5 hours. Afterward, 1ml of complete media was added, and the cells were incubated overnight. All incubation steps were done at 37°C with 5%CO_2.

Mast cell release and degranulation

Mouse bone marrow-derived mast cells were cultured from femurs of C57BL/6J mice as described (Jensen et al., 2006). Degranulation was assessed by measuring β-hexoseaminidase release as described (Cruse et al., 2013) using mast cells sensitized with 100ng/ml anti-DNP IgE (SPE7 clone) (Sigma Aldrich) for 16 hμrs, before the cells were challenged for 30 minutes with the indicated stimulus.

Calcium imaging on mast cells

Changes in cytosolic Ca^{2+} were assayed using ratiometric Fura-2 AM measurements as described (Cruse et al., 2013). Fluorescence was measured at two excitation wavelengths (340 and 380 nm) and an emission wavelength of 510 nm using a BioTek Neo2 multimode plate reader. The ratio of fluorescence readings was calculated following subtraction of background fluorescence of cells not loaded with Fura-2 AM.

Immunohistochemistry

DRGs were dissected from mice with various genotypes. Double and single IHC were performed as previously described (Mishra and Hoon, 2013). Images were collected on an Eclipse Ti (Nikon, Melville, NY) fluorescent microscope. Sections were selected randomly, and counting was performed on each DRG section and presented as mean of 3-5 sections from each mouse.

Quantification of periostin from mouse cell line

The murine keratinocyte cell line (Balb/MK2) was used in this study to determine the periostin production induced by TSLP. Cells were cultured in EMEM medium according to the previously described method (Fukuyama et al., 2018). Confluent cells were exposed to TSLP at 1 or 10ng/ml in FBS-free medium for 24 hr. Inhibitory effect of the JAK2 inhibitor, SD 1008 and the STAT3 inhibitor, niclosamide, on TSLP-induced periostin production was also quantified using the murine Balb/MK2 keratinocyte cell line. Confluent cells were pre-exposed for 4 hr to SD 1008 (10 μmol/l) or niclosamide (10 μmol/l), before being exposed to the TSLP at 10ng/ml for a further 24 hr. After TSLP exposure, periostin levels in cell supernatant were determined by ELISA according to the manufacturer's instructions.

Calcium imaging on mouse DRG neurons

Before imaging, cells were incubated in 350μL of complete media containing 5μM Fura-2 AM (Enzo) for 30 min at 37°C with 5%CO_2. During imaging, the cells were perfused with a buffer containing the following: 135mM sodium chloride, 3.2mM potassium chloride,

2.5mM magnesium chloride, 2.8mM calcium chloride, 667μM monobasic sodium phosphate, 14.2mM sodium bicarbonate, and 10.9mM D-glucose (all from VWR) with a pH between 7.00 and 7.40. The buffer and the holding plate were kept at 37°C while imaging. Imaging data was collected on a TE200 inverted microscope using NIS Elements software (Nikon). Cells were exposed to 340 and 380nm wavelengths for 100 ms and the A_{340}/A_{380} ratio was calculated. Traces were analyzed using Excel and responses greater than 10% of the baseline were counted. Each data point in the scatterplots represents one coverslip.

Whole-cell patch clamp recordings in DRG neurons

The mouse DRGs were removed aseptically from SOM-reporter mice (6-8 weeks) and incubated with collagenase (1.25mg/ml, Roche)/dispase-II (2.4 units/ml, Roche) at 37°C for 90 min, then digested with 0.25% trypsin for 8 min at 37°C, followed by 0.25% trypsin inhibitor. Cells were mechanically dissociated with a flame polished Pasteur pipette in the presence of 0.05% DNase I (Sigma). DRG cells were plated on glass coverslips and grown in a neurobasal defined medium (with 2% B27 supplement, Invitrogen) with 5 μM AraC and 5% carbon dioxide at 36.5°C. DRG neurons were grown for 24 hours before use. Whole-cell patch clamp recordings were performed at room temperature using an Axopatch-700B amplifier (Axon Instruments) with a Digidata 1440B (Axon Instruments). Only SST-positive neurons (< 20) were recorded. SST-negative neurons were also recorded as control. The patch pipettes were pulled from borosilicate capillaries (World Precision Instruments, Inc.) using a P-97 Flaming/Brown micropipette puller (Sutter Instrument Co.). The pipette resistance was 4-6 MΩ for whole-cell recording of periostin–induced inward currents, as previously recorded (Han et al., 2018). The internal pipette solution contains (in mM): 126 K-gluconate,10 NaCl, 1$MgCl_2$, 10 EGTA, 10 HEPES and 2Na-ATP (adjusted to pH 7.4 with KOH, Osmolority295-300 mOsm), and extracellular solution contains (in mM): 140 NaCl, 5 KCl, 2 $MgCl_2$, 2$CaCl_2$, 10 HEPES, 10 glucose, adjusted to pH 7.4 with KOH.

Reverse Transcription-PCR

RNA was isolated from fresh-frozen lumbar DRG from mice, dogs and NHP using RNA easy kit (QIAGEN, USA) according to the manufacturer protocol. To synthesize cDNA 200ng of RNA was used with 2μL random hexamer primers (Invitrogen) and SmartScribe Reverse Transcriptase (Clontech), as described previously (Mishra and Hoon, 2013). Taqman probes for all genes were purchased from Invitrogen. All samples were run on an Applied Biosystems StepOnePlus Real Time PCR System using Taqman Gene Expression Master Mix (Applied Biosystems, Cat # 4369016) with the recommended qPCR cycle. CT values were calculated using StepOne Software v2.2.2 (Applied Biosystems). GAPDH was used as a housekeeping gene for normalization. Relative tissue expression values were calculated using the following equation: relative expression = $2^{-\Delta CT}$.

Western blot (WB)

To extract total protein, dorsal root ganglia, and skin were homogenized using a tissue homogenizer in the presence of 100 μL of ice cold RIPA buffer supplemented with protease inhibitor tablets (Pierce). Total protein of lysates was measured using standard BCA (Bicinchoninic Acid Assay). Protein lysates were then denatured by heating at 95°C in Laemmli's buffer containing 2% w/v SDS, 62.5mM Tris (pH 6.8), 10% glycerol, 50mM DTT, and 0.01% w/v bromophenol blue. The lysates were cooled on ice and briefly micro-centrifuged. Aliquots of 35 μg of protein were loaded onto a 10% SDS-PAGE gel, and subsequently electro blotted onto PVDF membranes. Membranes were incubated in 15ml of blocking buffer (20mM Tris base and 140mM NaCl, 5% bovine serum albumin, and 0.1% Tween-20) for 1 hour. Membranes were then incubated with the desired primary antibody diluted in 10ml of blocking buffer at 4°C overnight. Next day membrane was washed and incubated with an appropriate horseradish peroxidase-conjugated secondary antibody (1:1000) to detect proteins in 10ml blocking buffer for 1-hr at room temperature. Immuno-reactive proteins were revealed using enhanced chemiluminescence detection (Pierce ECL). The densitometry analysis was performed using open sourced ImageJ software from NIH. Anti-TSLP receptor antibody was used at 1ng/ml. All other primary antibodies were used at a dilution of 1:1000. Secondary anti-rabbit and anti-mouse antibodies were purchased from Santa Cruz Biotechnology and used in 1:1000 dilution.

QUANTIFICATION AND STATISTICAL ANALYSIS

Statistical analyses and graphs were made in Prism 8 (GraphPad Software, La Jolla, CA). Differences between mean values were analyzed using unpaired one-tailed and two-tailed Student's t test as appropriate or 1-way/2-way analysis of variances (ANOVA) with Dunn's multiple comparisons post hoc test when more than two data groups were compared. Differences were considered significant for *$p < 0.05$. p values definition, and number of replicates as well as definitions of center and dispersion were given in the respective figure legend. No statistical method was employed to predetermine sample sizes. The sample sizes used in our experiments were similar to those generally used in the field.